Miner Deposita
DOI 10.1007/s00126-007-0143-5

ARTICLE

The composition of magmatic Ni–Cu–(PGE) sulfide deposits in the Tati and Selebi-Phikwe belts of eastern Botswana

W. D. Maier · S.-J. Barnes · G. Chinyepi · J. M. Barton Jr · B. Eglington · I. Setshedi

Received: 12 April 2006 / Accepted: 9 May 2007

Abstract We studied a number of magmatic Ni–Cu–(PGE) sulfide deposits in two distinct belts in eastern Botswana. The Tati belt contains several relatively small deposits (up to 4.5 Mt of ore at 2.05% Ni and 0.85% Cu) at Phoenix, Selkirk and Tekwane. The deposits are hosted by ca 2.7 Ga, low- to medium-grade metamorphosed gabbroic–troctolitic intrusions situated within or at the periphery of a greenstone belt. The deposits of the Selebi-Phikwe belt are larger in size (up to 31 Mt of ore grade). They are hosted by high-grade metamorphosed gabbronorites, pyroxenites and peridotites believed to be older than ca 2.0 Ga that intruded gneisses of the Central Zone of the Limpopo metamorphic belt. The composition of the sulfide mineralisation in the two belts shows systematic variation. Most of the mineralisation in the Tati belt contains 2–9% Ni and 0.05–4% Cu (Cu/Cu + Ni=0.4–0.7), whereas most of the mineralisation in the Selebi-Phikwe belt contains 1–3% Ni and 0.1–4% Cu (Cu/Cu + Ni=0.4–0.9). The Cu–Ni tenors of the ores in both belts are consistent with crystallization from a basaltic magma. The Tati ores contain mostly >3 ppm Pt + Pd (Pt/Pd 0.1–1), with Pd/Ir=100–1,000, indicative of a differentiated basaltic magma that remained S-undersaturated before emplacement. Most of the Selebi-Phikwe ores have <0.5 ppm Pt + Pd (Pt/Pd<0.1–1), with Pd/Ir=10–500. This suggests a relatively less differentiated magma that reached S saturation before emplacement. The Tati rocks show flat mantle-normalised incompatible trace element patterns (average Th/Yb_N=1.57), except for strong enrichments in large ion lithophile elements (Cs, Rb, Ba, U, K). Such patterns are characteristic of relatively uncontaminated oceanic arc magmas and suggest that the Tati intrusions were emplaced in a destructive plate margin setting. Most of the Selebi-Phikwe rocks (notably Dikoloti) have more fractionated trace element signatures (average Th/Yb_N= 4.22), possibly indicating digestion of upper crustal material during magma emplacement. However, as there are also samples that have oceanic arc-like signatures, an alternative possibility is that the composition of most Selebi-Phikwe rocks reflects tectonic mingling of the intrusive rocks with the country rocks. The implication is that orogenic belts may have a higher prospectivity for magmatic Ni–Cu ores than presently recognised. The trigger mechanism for sulfide saturation and segregation in all intrusions remains unclear. Whereas the host rocks to the intrusions appear to be relatively sulfur poor, addition of crustal S to the magmas is suggested by low Se/S ratios in some of the ores (notably at Selebi-Phikwe). External S sources may thus remain unidentified due to poor exposure and/or S mobility in response to metamorphism.

Keywords Nickel-copper deposits · Platinum-group elements · Phoenix · Selkirk · Selebi-Phikwe · Tekwane · Dikoloti · Botswana

Editorial handling: P. Lightfoot

W. D. Maier (✉)
Centre for Exploration Targeting, University of Western Australia, Crawley 6009, Australia
e-mail: wdmaier@cyllene.uwa.edu.au

S.-J. Barnes
Sciences Appliquées, Université du Québec à Chicoutimi, Chicoutimi, Canada G7H 2B1

G. Chinyepi · I. Setshedi
Department of Geology, University of Pretoria, Pretoria 0001, South Africa

J. M. Barton Jr
Department of Geology, Fort Hare University, Alice 5700, South Africa

B. Eglington
Department of Geology, University of Saskatchewan, Saskatoon, Canada

Introduction

The area to the east and south of Francistown, eastern Botswana hosts a number of intrusive magmatic Ni–Cu–(PGE) sulfide deposits that remain poorly characterised (Fig. 1). Several of the deposits are of considerable economic interest, including the active mines at Phoenix and Selebi-Phikwe and the Selkirk ore body. The deposits are of variable size ranging from 31 Mt of ore (1.36% Ni, 1.12% Cu) at Phikwe to 0.6 Mt of ore (1.2% Ni, 0.6% Cu) at Tekwane (Table 1). Some of the deposits, notably at Phoenix, contain important concentrations of platinum-group elements (ca 5–10 ppm in the sulfides). In the present paper, we provide an overview of the existing geological data and present new whole rock compositional data for the sulfide mineralised rocks. Based on our data, we reevaluate the paleotectonic setting of the intrusions, the nature of the magmas from which the ores precipitated, the

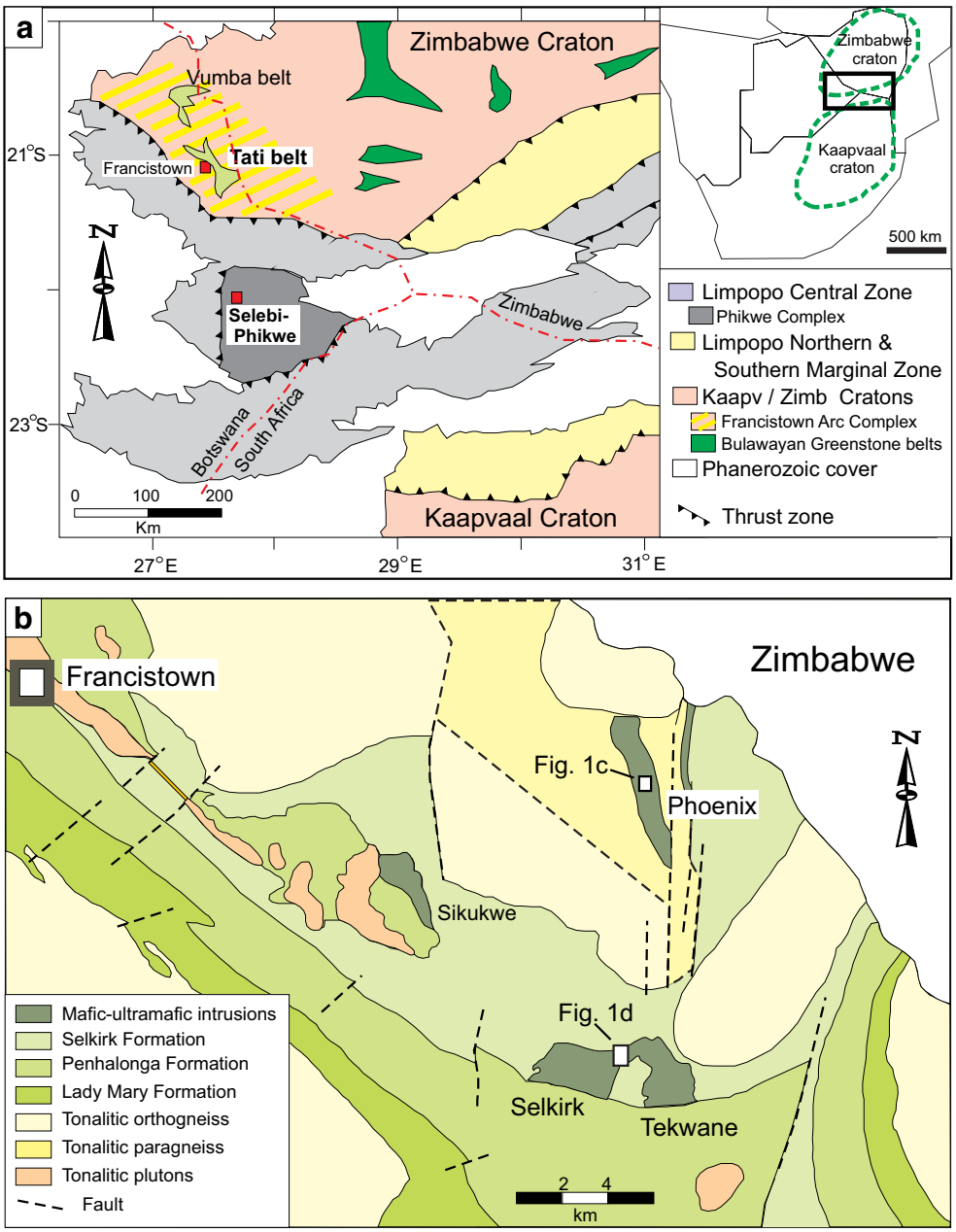

Fig. 1 **a** Schematic map of the Limpopo Belt and adjacent cratons showing studied localities. **b** Geological map of the central portion of the Tati greenstone belt indicating locality of Phoenix, Selkirk and Tekwane deposits. Figure modified after Johnson (1986). **c** Map of the Phoenix intrusion showing distribution of the ores (after Johnson 1986). **d** Map of part of the Selkirk intrusion (provided by Tati Nickel Company). **e** Schematic geological map of the Selebi-Phikwe area, with locations of deposits discussed in the text. Figure modified after Marsh (1978). **f** N–S section across Selebi-Phikwe Ni belt (along *dense stippled line* in **e**). Figure modified after Gallon (1986). **g** Section through Dikoloti deposit (after Brown 1988). See **e** for location of section

Fig. 1 (continued)

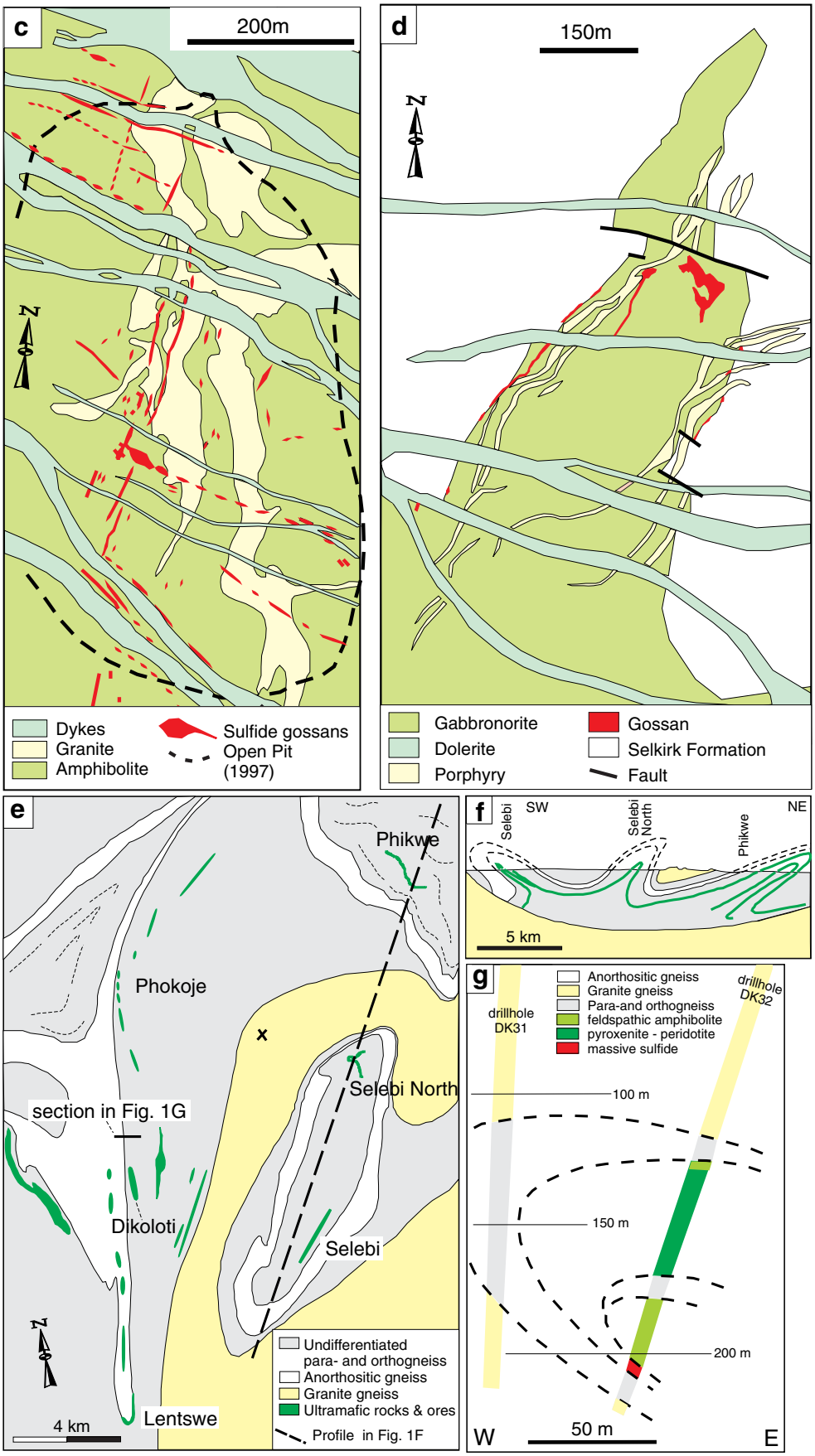

causes for sulfide saturation and segregation and the degree of modification that the ores underwent during tectonism and regional metamorphism.

Regional geology

General

The eastern Botswana Ni–Cu–(PGE) deposits may be subdivided into two groups. The first group of deposits, hosted by the Phoenix, Selkirk and Tekwane intrusions occurs within and in the periphery of the Tati greenstone belt (Fig. 1a–d). The deposits were discovered in 1963 by Sedge Botswana Ltd., a subsidiary of the Anglo American Corporation, based on mapping and stream sediment geochemistry. The second group of deposits, comprising Phikwe, Dikoloti, Lentswe and Phokoje, are hosted by the Selebi-Phikwe mafic–ultramafic intrusions that occur within gneisses of the Limpopo metamorphic belt some 200 km to the south of the Tati belt (Fig. 1a,e–g; Gordon 1973; Baldock et al. 1976). Most of the deposits were discovered by BCL (Bamangwato Concessions) between 1963 and 1966 using soil geochemistry.

Geology of the Tati greenstone belt

The Tati greenstone belt, together with the adjacent Vumba greenstone belt, forms part of the Francistown Arc Complex (Carney et al. 1994; McCourt et al. 2004) located along the southwestern margin of the Zimbabwe craton (Fig. 1a). Based on lithostratigraphic similarities, Carney et al. (1994) correlated the volcano-sedimentary rocks of the Francistown Arc Complex with the ca 2.7 Ga Upper Bulawayan greenstones in Zimbabwe (Fig. 1a). Bagai et al. (2002) dated tonalite–trondhjemite gneisses in the Vumba greenstone belt at 2,647±4 to 2,696±4 Ma (U-Pb SHRIMP age on zircon), and Van Geffen (2004) dated a gabbro at Phoenix Mine at 2,703±30 Ma (electron microprobe dating of monazite grains), consistent with this model.

The main lithologies within the Tati greenstone belt comprise lower greenschist to lower amphibolite facies volcanic and sedimentary rocks intruded by granitoids of unknown age (mainly tonalitic orthogneiss, tonalitic paragneiss, and post-tectonic tonalite–adamellite plutons; Fig. 1b). The volcano-sedimentary succession has been subdivided into three formations that contain a progressively higher proportion of felsic volcanic rocks with height (Key 1976). At the base is the <1,600 m Lady Mary Formation that consists mainly of altered komatiite and komatiitic basalt and lesser amounts of quartzitic schist, limestone and iron formation. The overlying >10-km-thick Penhalonga Formation consists of basaltic, andesitic and rhyolitic volcanics and volcaniclastic rocks, as well as phyllites, black shales (containing unspecified amounts of accessory pyrite, Key 1976, p 21), limestones and jaspilites. This is capped by the Selkirk Formation (>1 km thick) which consists mainly of dacitic and rhyolitic volcaniclastic rocks and minor amounts of mafic volcanic rocks, quartzites and quartz sericite schists. The Selkirk Formation also hosts the Phoenix, Selkirk and Tekwane meta-gabbronoritic intrusions and the Sikukwe meta-peridotite intrusion (Fig. 1b).

Geology of the Selebi-Phikwe area

The Selebi-Phikwe area forms part of the Limpopo Belt, an Archean to Paleoproterozoic ca 250×550-km granulite facies metamorphic belt situated between the Kaapvaal and Zimbabwe cratons (Barton et al. 2006 and references therein; Fig. 1a). The Limpopo Belt consists of several terranes with different formation ages (between 3.2 and ca 2.6 Ga) and tectonometamorphic histories. These terranes have been accreted onto the Zimbabwe and Kaapvaal cratons along wide, steeply dipping shear zones over a period of ca 700 Ma, from 2.7 to 2.04 Ga (Barton et al. 2006). The major terranes comprise the Central Zone, Southern Marginal Zone and Northern Marginal Zone. The Phikwe Complex is located within the Central Zone and largely consists of Archean hornblende-bearing tonalitic and trondhjemitic gneisses. It also contains the Selebi-Phikwe belt of mafic–ultramafic intrusions (Fig. 1a) that is hosted by medium- to coarse-grained, massive to weakly foliated, granoblastic to porphyroblastic granite gneiss and a variety of banded supracrustal gneisses comprising hornblende-gneiss, quartzofeldspathic gneiss and anorthositic gneiss. The protoliths to the hornblende gneisses are believed to be volcanics and shallow intrusions of tholeiitic basaltic and Ti-rich ferrobasaltic composition, whereas the protoliths to the quartzofeldspathic gneisses may have been calcalkaline volcano-sedimentary rocks (Brown 1988). Subordinate amounts of pelitic schists, marbles, impure quartzites and ironstones are also observed. Most of the above rocks are very sulfide poor (<200 ppm S; Brown 1988).

A few age determinations constrain relationships in the Selebi-Phikwe area. Samples of the granite gneisses have been dated at 2.6–2.65 Ga (U-Pb SHRIMP method; McCourt et al. 2004). According to Wright (1977) and Brown (1988), the granite gneisses have intrusive relationships with the supracrustal rocks, implying that the latter are older than ca 2.6 Ga. The absolute and relative ages of the mafic–ultramafic intrusions remain unclear, as lithological contacts are mostly tectonic. All that can be said is that they are older than ca 2.0 Ga.

Table 1 Estimated historic + current ore reserves of NE Botswana Ni–Cu deposits

	mt	Cu (%)	Ni (%)	Cu/Ni	Ni tenor (wt%)
Phoenix[a]	4.50	0.85	2.05	0.41	8–9
Selkirk[a]	3.30	0.81	0.93	0.87	3
Tekwane[b]	0.60	0.60	1.20	0.50	9.5
Phikwe[c]	31.00	1.12	1.36	0.82	2.6
Selebi[c]	12.60	1.50	0.74	2.03	na
Selebi North[c]	1.90	0.97	0.86	1.13	na
Dikoloti[d]	2.50	0.50	0.70	0.71	1.1
Lentswe[d]	1.50	0.40	0.50	0.80	na

[a] Johnson (1986)
[b] Key (1976)
[c] Gordon (1973)
[d] Brown (1988)

Description of the deposits

Tati greenstone belt

(1) Phoenix

The Phoenix deposit is located at the northern periphery of the Tati greenstone belt (Fig. 1b). The intrusion hosting the deposit crops out as an elongated, north-striking body ca 5 km long and 400 to 1,500 m wide, but its precise geometry is unknown. It consists of medium- to coarse-grained weakly deformed metagabbronorites (Fig. 2a) that have been pervasively altered to an assemblage of hornblende, albite, oligoclase, chlorite, epidote-sericite and quartz. The intrusion is cut by abundant late aplitic–pegmatitic veins of granitic composition (dated at 1,022± 16 Ma, U-Pb SHRIMP-II on zircon; Van de Wel et al. 1998) and by dolerites (Fig. 1c). The country rocks are tonalitic paragneisses that may sometimes contain accessory chalcopyrite (Key 1976).

The magmatic sulfide mineralisation occurs in disseminated, massive and vein-like form throughout the gabbronorites and, less commonly, in the granite (Fig. 2a–c). The disseminated sulfides form submillimetre- to centimetre-sized intergranular masses of pyrrhotite, chalcopyrite and pentlandite (Fig. 2a). The massive sulfides form a series of mostly relatively thin (up to 1.5 m) sub-vertical sheets and veins that may represent fissure and fracture fillings. They strike predominantly in N–S and E–W direction and occur throughout much of the open pit (Fig. 1c). The massive/vein-type sulfides show considerable compositional variation on a centimeter to meter scale. Most samples are dominated by pyrrhotite containing flame-like lamellae and granular aggregates of pentlandite, but chalcopyrite-rich (10–90% modal) massive/vein-type sulfides also occur. Accessory sulfides include sphalerite, molybdenite, galena and altaite (PbTe; Van Geffen 2004). Van Geffen (2004) also identified a number of platinum-group minerals in the ores, including merenskyite [$(Pd,Pt)(Bi,Te)_2$], hollingworthite [(Rh,Pt)AsS] and sperrylite ($PtAs_2$), as well as hessite (Ag_2Te), argentopentlandite [$Ag(Fe,Ni)_8S_8$], rheniite (ReS_2) and gold.

(2) Selkirk

The intrusion hosting the Selkirk deposit is located in the centre of the Tati greenstone belt near the contact between the Penhalonga and Selkirk Formations (Fig. 1b). The intrusion consists of medium-grained, layered metagabbronorite and anorthosite. It forms a ca 3×2-km wedge-shaped body (Fig. 1b) of unknown thickness (Key 1976; Johnson 1986) whose contact relationships with the volcano-sedimentary host rocks are poorly exposed. The main silicate minerals are sericite, chlorite and amphibole, representing the alteration products of plagioclase and pyroxene. Quartz is an accessory phase. Some samples show ophitic textures where narrow laths of altered plagioclase (up to 2 mm long) are included in altered pyroxene oikocrysts (up to 1 cm wide).

The intrusion hosts a ca 20-m-thick and up to ca 250-m-long lens of massive sulfide that is mantled by a zone of disseminated sulfides (ca 20 vol.%) of uncertain width. Pyrrhotite constitutes up to 90 vol.% of the massive ores. Pentlandite occurs as flame-like lamellae and granular aggregates in pyrrhotite. Chalcopyrite predominantly occurs in the disseminated sulfides (Fig. 2d). Magnetite locally constitutes up to 15% of the opaque fraction, occurring as subhedral grains that may be distinctly rounded. In some cases, pyrite may constitute ca 5% of the sulfides, forming late-stage veins and euhedral or subhedral crystals. The massive sulfides may also contain distinctly rounded silicate inclusions reminiscent of *durchbewegung* textures (Vokes 1969).

(3) Tekwane

Much of the information available on the geology and composition of the Tekwane intrusion is derived from unpublished company reports (e.g. summary report of the results from PL96/93; Falconbridge Ventures of Africa 1998). The body represents a 2.7×1.3-km-wide, 0.2- to 1.8-km-thick keel-shaped apophysis of the Selkirk intrusion (Gallery Gold Company, internal report, February 2002). Tekwane is relatively undeformed and forms a shallow synform plunging at a moderate angle (15°) to the south. Lithologies identified during drilling include an upper

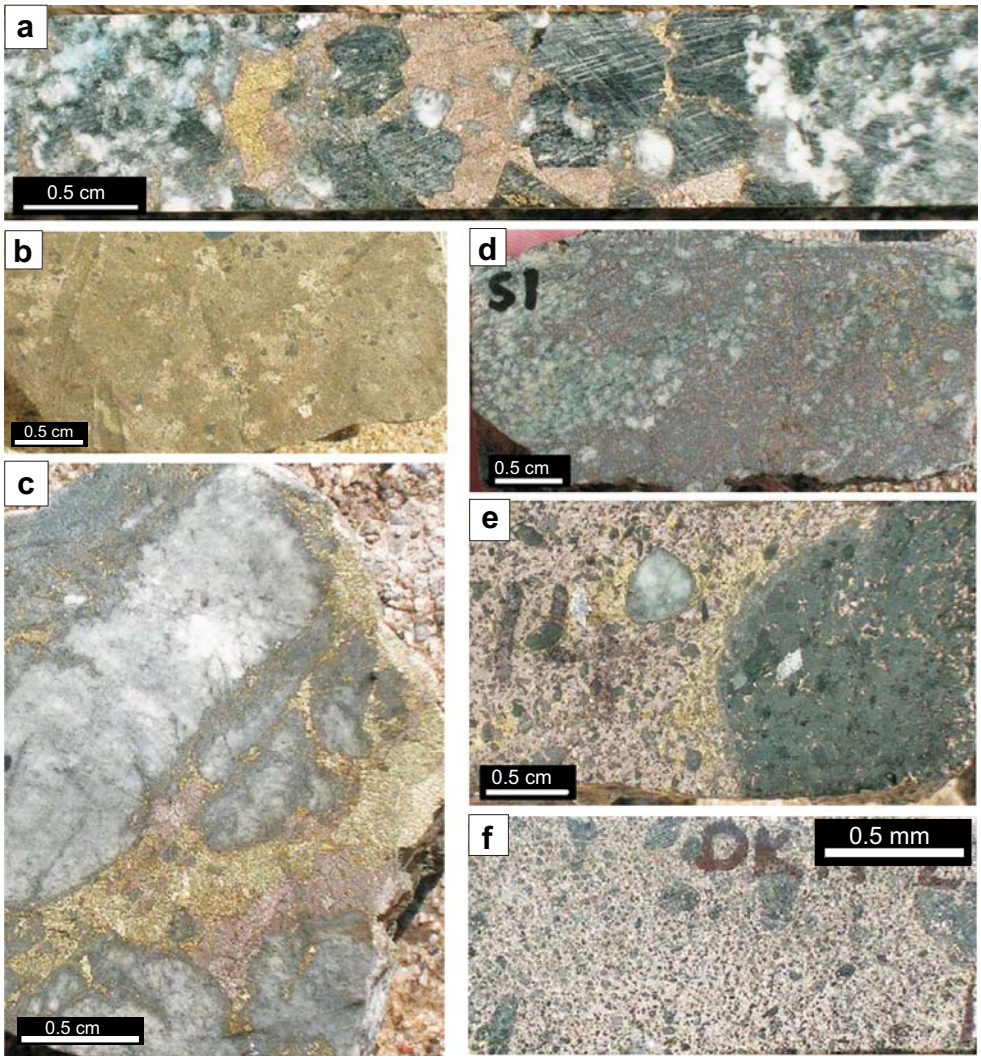

Fig. 2 Sulfide ores from the Tati and Selebi-Phikwe Belts. **a** Medium- to coarse-grained gabbronorite with disseminated sulfide mineralisation. Sample PS 148-215.76, Phoenix. **b** Massive pyrrhotite with granular pentlandite and small rounded silicate inclusions. Sample P10, Phoenix. **c** Chalcopyrite and pyrrhotite veins in gneiss. Sample P5, Phoenix. **d** Disseminated chalcopyrite–pyrrhotite ore collected 4 m below massive sulfide body. Sample S1, Selkirk. **e** Massive pyrrhotite ore containing rounded inclusions of silicate rocks and magnetite. Note concentration of chalcopyrite around large amphibolite inclusion on right. Sample SP13-1, Phikwe. **f** Semi-massive pyrrhotite ore with rounded silicate rock inclusions. Sample DK 17-2, Dikoloti

layered troctolite, a large mass of (olivine-) leucogabbronorite and a basal variable-textured gabbronorite. The mineralisation occurs in the form of up to ca 20-m-thick discontinuous lenses and layers of semi-massive and disseminated sulfides within the variable-textured basal gabbronorite, with peak grades of 0.96 ppm Pt + Pd + Au, 0.25% Ni and 0.16% Cu over 52 m. Analogous contact-style PGE mineralisation occurs in many mafic–ultramafic layered intrusions elsewhere in the world (see Maier 2005 and references therein). Pyrrhotite, pentlandite (occurring as flame-like exsolution lamellae in pyrrhotite) and chalcopyrite are the main sulfide phases. In our samples, they are finely intergrown with the silicates. Pyrite is locally abundant, forming relatively coarse-grained subhedra or veins and framboidal masses. Galena was occasionally observed in veins and at pyrite–pyrrhotite grain boundaries. Platinum-group minerals range in size from 2–10 μ and consist of Bi-kotulskite [$Pd(TeBi)_{1-2}$], sperrylite ($PtAs_2$), and michenerite [(Pd,Pt)BiTe]. Native gold, melonite ($NiTe_2$), hessite and cobaltite (CoAsS) were also observed.

Selebi-Phikwe belt

(1) Phikwe

The intrusion hosting the Phikwe deposit forms part of the Selebi-Phikwe belt of intrusions that also contain the Selebi, Selebi North, Dikoloti, Lentswe and Phokoje deposits (Fig. 1e–g). In all these deposits, the sulfide ores are mainly associated with boudinaged lenses and layers of fine- to medium-grained amphibolite interlayered with various types of gneisses (Gordon 1973; Wakefield 1976; Key 1976; Gallon 1986; Brown 1988). The ore-bearing intrusions are generally relatively thin (e.g. on average 11 m in the Phikwe area; Lear 1979), but this may largely be the result of intense folding and shearing. The amphibolites consist mainly of hornblende, feldspar, gedrite and mica. Minor metamorphic orthopyroxene and olivine also occur. Based on whole rock compositional data and CIPW norms of a large number of samples, Brown (1988) estimated that the parental magmas to the intrusions were tholeiitic basalts (with ca 8 wt% MgO) that crystallised

variable proportions of olivine (Fo_{85}), pyroxene (En_{85}) and plagioclase (An_{83}).

Disseminated and massive sulfides occur throughout the amphibolites, locally forming up to 38-m-thick massive and semi-massive concentrations, particularly near the contacts between the amphibolites and the host gneisses (Fig. 1g). The sulfides are intensely tectonised, as evidenced by their concentration in crosscutting veins and fold closures, common *durchbewegung* fabrics, and the concentration of silicate inclusions (Fig. 2e,f) along traces of isoclinal folds within the massive sulfides. This suggests that the massive sulfides acted as zones of at least three phases of shearing resulting in intense tectonisation (Brown 1988). Pyrrhotite, pentlandite and chalcopyrite are the main sulfide minerals and occur in variable relative proportions within individual samples of massive and disseminated ore. Chalcopyrite may be relatively concentrated around and within silicate inclusions (Fig. 2e). Minor sulfides formed during hydrothermal and supergene alteration include bravoite, marcasite, pyrite and violarite (Lear 1979). Magnetite constitutes up to 20 vol.% of the opaque fraction in the form of euhedral, subhedral or anhedral grains (Fig. 2e).

(2) Dikoloti-Lentswe-Phokoje

The Dikoloti, Lentswe and Phokoje deposits have been described in some detail by Marsh (1978) and Brown (1988) from which most of the following description is taken. The deposits are located a few kilometres to the SW and W of the Selebi-Phikwe deposits (Fig. 1e). They occur within tectonised lenses and layers of partially serpentinised/amphibolised peridotite, pyroxenite and melagabbronorite that may reach a thickness of 45 m. The intrusions are hosted by hornblende gneiss, quartzofeldspathic gneiss and magnetite quartzite. Based mainly on whole rock major element data, CIPW norms and Cu/Ni ratios, Brown (1988) suggested that the Dikoloti, Lentswe and Phokoje intrusions crystallised from magma of broadly similar composition as the Phikwe intrusions, but contain a larger cumulate component. Based on lithostratigraphic correlations, he went on to propose that the Dikoloti, Lentswe and Phokoje bodies intruded at a higher stratigraphic level than the Phikwe intrusions. However, as the contacts between the mafic–ultramafic intrusions and the gneissic host rocks tend to be intensely sheared, lithostratigraphic reconstructions are contentious, and other authors have favoured a model whereby all intrusions in the Selebi-Phikwe belt belong to the same tectonically dismembered sill (Gordon 1973).

Sulfides occur in disseminated form and occasionally as thin (<1 m) irregular massive lenses, the latter situated particularly along the basal and upper contacts of the intrusions. Concentrations of massive sulfides also tend to occur in the nose and adjacent limbs of isoclinal antiforms, e.g. at Dikoloti (Fig. 1g). In some cases, massive sulfide lenses can reach a width of 10 m. As was observed at Phikwe, the sulfides contain abundant silicate inclusions consisting of hornblende, biotite, carbonate, epidote and chlorite (Fig. 2f). Pyrrhotite is the main sulfide mineral. Pentlandite (occurring mainly as flame-like exsolutions in pyrrhotite) and chalcopyrite are significantly less abundant than at Phikwe (<5 vol.%). Magnetite makes up ~5 vol.% of the massive ore but >10 vol.% of the disseminated ore. Both the magnetite and the silicate inclusions may be distinctly rounded.

Analytical techniques

Fourty grab and borehole samples were jaw-crushed and then pulverised in a C-steel mill at the University of Pretoria. The mill has been tested to verify that it does not contaminate the samples with PGE. Depending on the size of the samples and the grain size, between 200 and 400 g of rock was pulverised. Concentrations of all elements were determined in the geochemical laboratory of the Université du Québec à Chicoutimi (UQAC). Sulfur was determined by combustion iodometric procedure, and the relative standard deviation in samples containing >0.1% sulfur is approximately 3%. Copper was determined by atomic absorption, and the relative standard deviation is approximately 4% in samples containing >0.1% sulfur. The PGE and Au were determined by instrumental neutron activation analysis (INAA) after preconcentration in a Ni sulfide bead (see Bédard and Barnes 2002 for analytical details) and sample irradiation at Ecole Polytechnique, Montreal. Analytical precision and accuracy are given in Table 2. A large number of other elements were also determined by INAA (Tables 3 and 4) partly because determination of major elements (Al_2O_3, Fe_2O_3, MgO, Na_2O, K_2O) by INAA permits the analysis of sulfide rich rocks that are difficult to analyse by X-ray fluorescence (XRF). Results for some elements, (Si, Ca, P and Zr) are not available because these elements are not well activated by neutron irradiation. The relative standard deviation on the in-house standard for all analysed elements (except Ag and Zn) is 2–5% (Table 3). The UQAC laboratory participates in the International Association of Geoanalysts' proficiency tests, a quality control program established to ensure the precision and accuracy of analyses. Results from the proficiency tests show that the difference between major elements as determined by INAA and the certified true values are less than five relative percent. Volatile contents of the samples have not been determined mainly because roasting of sulfidic samples may result in significant oxygen gain. The XRF data of Brown (1988) and Key (1976) suggest that the Phikwe amphibolites show mostly between 1 and 3% loss on ignition (L.O.I.), and the Selkirk and Tekwane gabbronorites show 2–5% L.O.I.

Table 2 Comparision of recommended PGE and Au values and those obtained at University of Quebec, Chicoutimi

Sample laboratory	SARM-7		SARM-7		Ax90		Ax90		Blank	
	UQAC n=5	+/−	Certified values[a]	+/−	UQAC	+/−	UQAC	+/−		+/−
		1 sigma			Accepted[b]	Sigma	This run n=2	Sigma	This run	Sigma
Os (ppb)	65	4	63	6.8	2.9	0.23	3.06	0.29	<0.5	0.5
Ir	83	3	73	12	3.23	0.12	3.31	0.07	<0.06	0.03
Ru	418	21	430	57	12.8	1.17	21.48	0.13	<6	5
Rh	239	4	230	13	11.74	0.50	13.16	1.46	<0.5	0.6
Pt	4,069	366	3,740	45	148	8.41	139.20	4.55	<5	5
Pd	1,510	33	1,530	32	360	14.84	347.69	16.79	<4.5	2
Au	364	51	310	15	5.1	0.44	4.97	0.58	0.1	0.1

[a] Steele et al. (1975)
[b] average Ax90 values 2002–2006 n=53

Table 3 Precision and accuracy of INAA analyses at UQAC (using in-house standard KPT-1)

KPT-1	Conc	RDS
Al_2O_3 (wt%)	14.78	1.4
Fe_2O_3	12.49	2.9
MgO	4.25	9.3
TiO2	0.91	2.1
MnO	0.15	1.0
Na_2O	2.52	1.9
K_2O	1.72	53.9
As (ppm)	2.24	16.2
Ba	469	4.9
C	1,811	11.0
Ce	63.8	2.1
Co	75	1.8
Cr	147	2.0
Cs	4.18	4.6
Cu (AA)	1,231	5.9
Eu	1.32	3.0
Hf	4.34	4.3
La	26.3	2.1
Lu	0.41	1.6
Nd	24.97	7.2
Ni	1,141	9.1
Rb	60	7.7
S	11,311	2.8
Sb	11	3.8
Sc	24	1.8
Se	2.7	12.0
Sm	4.94	2.7
Ta	0.54	21.2
Tb	0.73	11.4
Th	7.65	3.0
U	1.74	6.3
V	220	1.3
Yb	2.71	2.8
Zn	112	13.1
Au (ppb)	50.97	24.3

Geochemistry

Lithophile elements

To be able to compare samples with variable sulfide contents, the concentrations of the lithophile elements have been recalculated on a sulfide-free basis. However, the original data are shown in Table 4.

The samples from the Selebi-Phikwe belt are gabbronorites, pyroxenites and peridotites with MgO contents between 6 and 29 wt% (Fig. 3). The bulk of the amphibolites plot between tie tielines from plagioclase to clinopyroxene and orthopyroxene, indicating that the samples were originally of gabbronoritic composition. The Dikoloti and Lentswe samples plot between the orthopyroxene and olivine fields, indicating that they were feldspathic peridotites. The analysed mafic–ultramafic intrusive rocks from the Tati belt are all amphibolites with MgO contents in the 6- to 13-wt% range. Their composition broadly overlaps with those of the Selebi-Phikwe amphibolites indicating that the protoliths to the Tati amphibolites were also gabbronorites. Most of the samples contain 15 to 22% Al_2O_3, and thus, they would have contained 50 to 75% plagioclase making them meso- to leucogabbronorites.

The incompatible trace element contents of most samples from both belts suggest that the rocks are cumulates. For example, Hf contents in the analysed amphibolites are <0.5 ppm, whereas typical oceanic and continental tholeiites contain between 1 and 7 ppm Hf (see compilation in Wilson 1989). Sample SP13-1 (from Phikwe) has markedly higher trace element contents than the other Phikwe samples, and thus, appears to represent the composition of a liquid. It consists of an amphibolite boulder within massive sulfide (Fig. 2e), containing 14.2 wt % Al_2O_3 and 8 wt% MgO. The major element contents

Table 4 Compositional data from NW Botswana Ni–Cu–(PGE) deposits

	Sulfide-poor mafic–ultramafic rocks					Granite			Disseminated sulfides
Sample	LT-7	148–247.2	148–237.3	148–100.8	148–191.6	148–270.3	119–222	148–261.2	DK–17
Rock type	per	gn	gn	gn	gn				
Belt	SP	Tati	Tati	Tati	Tati	Tati	Tati	Tati	SP
Deposit	Lentswe	Phoenix	Phoenix	Phoenix	Phoenix	Phoenix	Phoenix	Phoenix	Dikoloti
TiO2 (wt%)	0.08	0.17	0.44	0.17	0.13	0.18	0.21	0.19	0.34
Al2O3	4.71	15.14	16.22	17.47	16.44	15.75	14.03	15.42	5.58
Fe2O3	14.77	9.05	6.48	6.43	6.47	2.17	3.03	1.80	4.31
MnO	0.18	0.18	0.13	0.12	0.13	0.04	0.05	0.03	0.05
MgO	29.58	8.67	10.30	10.73	11.37	0.75	0.49	0.68	17.68
Na2O	0.07	2.34	1.49	1.35	1.33	4.36	3.65	3.96	0.27
K2O	0.20	0.37	0.23	0.15	1.39	0.77	0.39	1.57	2.20
FeS	0.00	0.00	0.00	0.19	0.00	0.00	4.05	1.17	16.11
S	0.04	0.03	0.03	0.16	0.02	0.01	2.94	0.95	11.11
% sulfide	<0.1	<0.1	<0.1	0.35	<0.1	<0.1	6.99	2.12	27.22
Ba (ppm)	9	66	26	44	237	312	217	446	49
Cl	85	<45	138	96	56	72	45	138	178
Cs	1.83	0.85	1.05	1.11	3.55	1.01	1.06	1.12	11.56
Hf	0.08	0.21	0.47	0.39	0.27	1.87	1.69	1.58	1.27
Rb	26	10	16	10	49	22	13	44	145
Sc	12.6	33.0	29.8	22.8	25.5	2.5	2.3	2.1	10.8
Ta	<0.02	0.09	0.06	0.04	<0.02	0.23	0.14	0.24	0.26
Th	0.06	0.14	0.23	0.25	0.04	2.93	1.93	2.12	0.48
U	0.06	0.22	<0.1	0.09	<0.05	0.97	0.54	1.02	0.36
La	0.29	0.86	1.24	1.13	0.51	13.11	8.60	11.26	4.20
Ce	<1	1.7	3.2	2.5	2.0	24.1	15.0	19.4	9.6
Nd	<1	0.91	2.47	<1	<1	7.59	4.63	6.43	4.21
Sm	0.04	0.36	0.70	0.42	0.26	1.24	0.83	1.11	0.97
Eu	0.01	0.20	0.23	0.25	0.18	0.56	0.49	0.52	0.17
Tb	0.02	0.11	0.21	0.13	0.07	0.13	0.07	0.12	0.12
Ho	0.02	0.36	0.37	0.20	0.24	0.26	0.19	0.73	0.26
Yb	0.08	0.49	0.77	0.45	0.37	0.35	0.26	0.36	0.41
Lu	0.02	0.09	0.12	0.07	0.06	0.06	0.04	0.06	0.08
Cr	1,840	289	780	782	607	10	16	8	1,534
V	62	197	173	128	127	20	30	22	69
Zn	142	62	39	49	39	29	45	38	64
Ni	540	144	216	644	245	22	5,051	1,904	2,887
Cu	392	188	103	341	25	10	3,333	2,959	10,666
Re	2.1	0.6	0.6	1.2	<0.3	0.2	26.9	0.3	6.0
Ag	<2	<2	<2	<2	<2	<2	<2	2.7	3.0
As	<0.5	<0.5	<0.5	0.3	<0.5	0.4	<0.5	0.8	<0.5
Co	76	48	37	45	41	6	164	34	171
Sb	<0.05	0.04	0.07	0.09	0.11	0.08	0.17	0.16	0.17
Se	<0.2	<0.2	<0.2	0.78	<0.2	0.92	11.34	4.18	3.17
Os (ppb)	<2	<2	<2	<2	<2	<2	1	<2	<2
Ir	0.63	0.10	0.08	0.55	0.24	<0.03	0.77	0.08	4.03
Ru	<7	4	<7	<7	<7	<7	<7	<7	<7
Rh	4.2	1.2	1.1	3.4	1.3	<0.3	50.0	1.7	21.4
Pt	10	9	13	47	22	<1.9	154	226	81
Pd	61	11	29	162	25	4	809	979	488
Au	3.7	1.3	1.2	11.3	0.5	0.2	32.2	34.3	38.1

Table 4 (continued)

	Disseminated sulfides									
Sample	SP-21	Sp13-1	SP-9	112–733	148–215.9	148–196.3	148–135.4	148–156.7	148–162.4	S8
Rock type										
Belt	SP	SP	SP	SP	Tati	Tati	Tati	Tati	Tati	Tati
Deposit	Phikwe	Phikwe	Phikwe	Phokoje	Phoenix	Phoenix	Phoenix	Phoenix	Phoenix	Selkirk
TiO2 (wt%)	nd	0.24	0.33	0.14	0.91	0.20	0.18	0.24	0.17	0.19
Al2O3	nd	13.2	22.52	14.38	6.66	15.91	15.26	12.69	16.94	17.07
Fe2O3	4.95	16.48	10.39	8.88	0.00	5.94	6.75	5.67	6.03	6.09
MnO	nd	0.36	0.18	0.16	0.08	0.11	0.13	0.12	0.13	0.12
MgO	nd	7.92	6.13	11.67	7.66	9.89	12.22	9.40	9.19	9.43
Na2O	0.77	1.24	0.72	1.18	0.52	0.94	0.95	1.20	1.55	0.70
K2O	nd	0.29	3.4	0.14	<0.1	1.25	0.20	0.57	0.45	<0.1
FeS	18.32	3.84	0.92	7.86	21.48	1.74	0.75	5.00	1.14	5.26
S	13.66	3.31	0.64	5.39	16.48	1.68	0.59	3.75	0.87	3.62
% sulfide	31.98	7.15	1.56	13.25	37.96	3.42	1.34	8.75	2.01	8.88
Ba (ppm)	14	7	377	8	<30	102	27	39	50	48
Cl	<40	478	386	394	35	43	39	64	67	55
Cs	<0.1	<0.1	6.46	<0.1	0.39	2.62	2.34	1.88	1.85	0.10
Hf	0.18	0.46	0.49	0.30	0.46	0.27	0.31	0.21	0.17	0.25
Rb	<2	9	175	9	<2	45	9	18	16	<7
Sc	13.1	16.9	12.5	10.8	25.9	27.2	23.5	31.0	28.3	12.8
Ta	<0.02	0.32	0.04	0.05	0.08	0.02	0.03	<0.02	0.02	0.02
Th	0.23	0.39	0.36	0.34	0.17	0.14	0.20	0.28	0.07	0.08
U	<0.1	0.36	0.10	<0.1	0.26	0.11	0.07	<0.1	<0.1	<0.04
La	1.29	4.95	2.53	1.36	0.85	1.12	1.06	0.84	0.94	0.70
Ce	2.3	17.5	4.2	2.0	1.0	2.5	2.7	2.2	1.8	1.7
Nd	1.00	6.07	2.65	<1	<1	1.30	<1	<1	<1	<1
Sm	0.31	2.42	0.76	0.52	0.48	0.48	0.42	0.52	0.46	0.38
Eu	0.24	0.85	0.36	0.27	0.08	0.25	0.22	0.20	0.23	0.22
Tb	<0.1	0.52	0.24	<0.1	<0.05	0.11	0.12	0.13	0.14	0.10
Ho	<0.32	0.70	0.20	<0.18	0.88	0.22	0.19	0.22	0.17	0.19
Yb	0.34	1.77	0.45	0.35	0.53	0.42	0.44	0.51	0.54	0.44
Lu	0.07	0.30	0.07	0.08	0.08	0.08	0.08	0.09	0.08	0.07
Cr	230	166	154	269	537	829	972	478	280	897
V	<10	213	86	103	200	140	124	156	148	87
Zn	101	174	162	72	51	54	42	58	40	126
Ni	5,511	1,322	801	3,665	39,291	1,725	1,668	7,100	1,952	2,858
Cu	33,588	17,400	249	2,912	9,434	11,373	1,100	6,263	1,556	2,090
Re	12.8	0.5	<0.3	13.2	59.1	14.3	5.1	29.6	5.2	8.4
Ag	13.4	3.4	<2	<2	3.7	3.2	<2	2.7	<2	<2
As	<0.5	0.4	<0.5	<0.5	<0.5	<0.5	<0.5	<0.5	<0.5	0.7
Co	347	86	53	189	759	69	75	204	70	159
Sb	<0.05	0.06	0.08	<0.05	0.24	0.15	0.18	0.16	0.15	0.46
Se	11.55	3.64	<2	3.73	40.66	5.05	2.77	14.42	3.27	7.06
Os (ppb)	<2	<2	<2	<2	11	<2	<2	4	<2	<2
Ir	1.98	0.32	0.03	1.15	14.52	2.12	0.91	3.71	0.49	0.79
Ru	<7	<7	<7	<7	17	<7	17	9	10	7
Rh	2.8	<0.3	<0.3	2.1	231	24.8	7.8	49.2	7.8	9.3
Pt	<40	124	7	36	1,722	246	140	373	140	125
Pd	18	24	7	13	8,235	1,094	551	1,614	565	500
Au	104.4	65.4	1.3	4.3	215.8	69.4	33.2	66.0	15.2	20.5

							Massive sulfides		
S1	S11	S2	S3	S6	TW-9	TW-7	DK-17-2	SP-13b	SP-18
Tati Selkirk	Tati Selkirk	Tati Selkirk	Tati Selkirk	Tati Selkirk	Tati Tekwane	Tati Tekwane	SP Dikoloti	SP Phikwe	SP Phikwe
0.15	0.53	0.10	0.45	0.28	0.31	0.21	nd	nd	nd
18.60	18.50	17.12	15.32	17.62	19.94	20.84	nd	nd	nd
6.42	10.83	6.20	6.06	2.65	5.37	5.63	1.33	0.00	0.00
0.13	0.21	0.13	0.16	0.17	0.11	0.11	nd	nd	nd
5.97	8.82	6.49	7.01	8.36	8.14	8.38	nd	nd	nd
1.56	0.25	1.09	0.64	1.66	1.10	1.03	0.22	0.14	0.25
1.21	<0.1	<0.1	2.16	0.16	<0.2	0.17	nd	nd	nd
7.75	1.52	9.16	1.52	7.89	1.68	1.63	30.70	48.31	42.95
5.35	1.09	6.56	1.14	5.35	1.31	1.42	20.48	30.71	28.67
13.10	2.61	15.72	2.66	13.24	2.99	3.05	51.18	79.02	71.62
412	<10	66	780	28	<10	5	<10	<30	<30
<33	<37	47	37	168	89	89	<40	65	<40
0.77	<0.1	0.12	0.93	0.12	0.55	0.38	0.58	<0.1	<0.1
0.26	0.88	0.16	0.65	0.27	0.20	0.23	0.72	<0.15	0.68
40	<2	<7	55	<7	<2	<2	<2	16	19
12.13	16.57	9.45	18.95	14.03	13.41	10.85	7.00	1.03	2.19
<0.02	0.12	<0.02	0.08	0.02	0.02	0.02	0.07	0.06	0.33
<0.02	0.23	<0.02	0.18	0.04	0.09	0.03	1.32	2.66	2.52
<0.02	0.16	<0.02	0.20	<0.04	<0.1	<0.1	0.54	0.56	2.22
0.19	1.90	0.20	3.00	1.00	0.78	0.56	4.33	2.18	2.41
<1	4.4	<1	7.2	2.7	1.1	1.6	9.8	4.0	<1
<1	2.43	<1	2.90	<1	<1	<1	2.84	<1	<1
0.19	1.15	0.19	1.21	0.52	0.50	0.44	1.17	0.37	0.76
0.13	0.44	0.11	0.39	0.29	0.36	0.37	0.36	0.65	0.73
0.05	0.29	0.06	0.25	0.13	0.12	0.08	0.14	<0.1	0.14
0.12	0.50	0.08	0.46	0.17	0.37	0.21	0.30	<0.54	0.35
0.27	1.11	0.27	0.83	0.57	0.58	0.55	0.51	<0.1	0.44
0.05	0.18	0.05	0.15	0.10	0.08	0.08	0.07	0.05	0.13
4,090	522	1,477	409	706	676	135	2,777	50	53
131	156	88	145	87	69	72	<10	124	<10
760	302	479	135	236	51	47	312	77	62
4,829	1,271	4,927	1,099	2,675	3,042	2,725	5,465	1,7518	1,7748
3,165	1,336	9,708	2,588	2,371	2,518	6,100	3,686	2,769	12,116
21.6	1.9	19.7	2.2	6.5	4.5	8.2	12.1	26.0	32.4
<2	<2	3.0	<2	<2	<2	<2	<2	<2	3.2
13.4	10.9	1.3	10.4	0.3	<0.5	1.1	<0.5	<0.5	<0.5
221	75	238	72	147	81	72	343	872	726
1.32	2.11	1.36	0.16	0.40	0.20	0.33	<0.05	<0.05	<0.05
8.36	2.35	10.76	3.43	5.70	2.95	4.46	6.29	103	27.89
<2	<2	<2	<2	<2	<2	<2	<2	<2	<2
2.16	0.31	2.27	0.34	0.69	0.78	1.96	4.62	2.04	1.70
9	3	4	3	8	<7	<7	<7	<7	<7
27.5	2.5	26.8	4.1	9.2	12.1	23.4	37.8	3.7	3.4
188	78	182	90	143	162	283	110	20	9
681	287	819	439	526	816	1,483	1,097	83	44
10.9	7.2	36.7	31.2	19.4	182.6	250.1	5.9	13.6	43.0

Table 4 (continued)

	Massive sulfides									
Sample	SP-16	112–738	P3	119–217.14	P8	P10	P4	P6	P1	119–217.3
Rock type										
Belt	SP	SP	Tati	Tati	Tati	Tati	Tati	Tati	Tati	Tati
Deposit	Phikwe	Phokoje	Phoenix	Phoenix	Phoenix	Phoenix	Phoenix	Phoenix	Phoenix	Phoenix
TiO2 (wt%)	nd	nd	<0.06	<0.16	<0.02	0.05	<0.02	0.02	<0.02	0.04
Al2O3	nd	nd	0.03	0.64	0.29	0.05	0.00	0.28	0.01	0.69
Fe2O3	0.00	0.00	0.00	0.00	0.00	0.00	0.00	0.00	0.00	0.00
MnO	nd	nd	0.00	0.02	0.01	0.01	0.00	0.01	0.00	0.02
MgO	nd	nd	<0.1	<0.19	0.06	<0.1	<0.1	0.20	<0.1	0.11
Na2O	0.53	0.17	0.00	0.11	0.02	0.01	0.00	0.01	0.00	0.11
K2O	nd	nd	<0.1	<0.1	<0.1	<0.1	<0.1	<0.1	<0.1	<0.1
FeS	38.01	44.39	41.53	30.82	52.45	51.93	51.14	50.95	52.69	49.84
S	26.03	30.29	33.83	31.38	36.19	36.01	35.66	35.48	35.29	33.9
% sulfide	64.04	74.68	75.36	62.20	88.64	87.94	86.80	86.43	87.98	83.74
Ba (ppm)	104.24	<30	<30	<30	<30	<30	<30	<30	<30	<30
Cl	<40	<40	31	30	30	38	29	41	23	52
Cs	<0.1	<0.1	<0.1	0.24	<0.1	<0.1	<0.1	<0.1	<0.1	<0.1
Hf	0.60	0.16	<0.15	<0.15	<0.15	<0.15	<0.15	<0.15	<0.15	<0.15
Rb	12	<2	<2	<2	<2	<2	<2	<2	<2	<2
Sc	2.77	3.90	0.22	0.67	0.42	0.33	0.11	0.46	0.05	0.69
Ta	0.31	<0.02	0.13	<0.02	<0.02	<0.02	0.05	<0.02	0.15	0.08
Th	3.61	0.13	<0.02	<0.02	<0.02	<0.02	<0.02	<0.02	<0.02	0.23
U	1.88	<0.1	<0.1	<0.1	<0.1	<0.1	<0.1	<0.1	<0.1	<0.1
La	4.95	0.39	<0.04	0.60	<0.04	<0.04	<0.04	<0.04	<0.04	0.90
Ce	9.7	<1	<1	<1	<1	<0.82	<1	<1	<1	<1
Nd	<1	<1	<1	<1	<1	<1	<1	<1	<1	<1
Sm	1.19	0.21	<0.01	0.07	0.03	<0.01	<0.01	0.01	<0.01	0.13
Eu	0.65	0.77	<0.05	<0.05	<0.05	<0.05	<0.05	<0.05	<0.05	<0.05
Tb	0.20	<0.1	<0.05	<0.05	<0.05	<0.05	<0.05	<0.05	<0.05	<0.05
Ho	0.45	<0.45	<0.1	<0.1	<0.1	<0.1	<0.1	<0.1	<0.1	<0.1
Yb	0.52	<0.1	<0.06	<0.06	<0.06	<0.06	<0.06	<0.06	<0.06	<0.06
Lu	0.17	0.02	<0.01	<0.01	<0.01	<0.01	<0.01	<0.01	<0.01	<0.01
Cr	53	54	147	84	25	54	51	158	73	90
V	<10	<10	22	14	14	170	9	59	11	15
Zn	78	157	325	221	35	21	27	19	42	163
Ni	14,542	20,309	38,811	10,461	79,338	68,424	69,531	69,060	77,894	66,619
Cu	23,990	390	140,206	282,653	363	505	18,265	283	21,165	1,782
Re	22.4	12.7	484	204	182	299	581	418	585	578
Ag	6.1	<2	24.4	123	<2	<2	<2	<2	<2	<2
As	<0.5	0.9	0.9	1.0	1.5	0.7	<0.5	<0.5	<0.5	<0.5
Co	743	970	1,046	324	1,896	1,789	1,904	1,297	2,143	1,898
Sb	<0.05	<0.05	<0.05	0.17	<0.05	<0.05	<0.05	<0.05	0.04	0.16
Se	24.19	43.10	83.63	66.78	115	80.26	81.41	98.66	88.95	72.11
Os (ppb)	<2	<2	18	<2	<2	<2	23	5	17	18
Ir	1.24	0.11	42.30	<0.03	7.08	17.43	66.13	22.14	54.59	48.00
Ru	<7	<7	91	<7	53	33	121	49	102	87
Rh	2.9	1.5	357	<1	200	397	783	678	817	827
Pt	9	15	208	<1.5	122	53	25	437	<28	619
Pd	29	167	4,809	435	8,430	5,565	5,974	5,923	7,248	5,851
Au	20.7	6.8	301	<0.01	9.2	12.8	81.5	10.2	64.2	92.5

						Vein sulfides		
P2	S12	233–13.3	S13	S9	S4	P5	P7	P9
						Granite	gn	gn
Tati	Tati	Tati	Tati	Tati	Tati	Tati	Tati	Tati
Phoenix	Selkirk	Selkirk	Selkirk	Selkirk	Selkirk	Phoenix	Phoenix	Phoenix
0.01	0.08	0.04	0.15	0.05	0.02	0.24	0.15	0.22
0.04	0.01	0.00	0.38	0.01	0.03	9.88	10.51	10.04
0.00	0.00	0.00	0.00	0.00	0.00	0.87	2.40	3.67
0.01	0.03	0.01	0.08	0.05	0.02	0.04	0.07	0.09
<0.1	<0.1	<0.1	0.28	<0.1	<0.1	1.50	3.58	5.22
<0.003	0.01	0.01	0.01	0.01	0.01	2.01	0.06	0.76
<0.1	<0.1	<0.1	<0.1	<0.1	<0.1	0.10	<0.1	<0.1
50.81	57.94	53.52	49.66	54.72	55.90	14.50	18.81	19.10
35.28	32.6	35.16	35.58	33.91	36.47	12.54	15.26	16.76
86.09	90.54	88.68	85.24	88.63	92.37	27.04	34.07	35.86
<30	<30	<30	<30	<30	<30	13	<10	15
41	19	33	23	41	31	55	47	104
<0.1	<0.1	<0.1	<0.1	<0.1	<0.1	0.55	<0.1	0.11
<0.15	<0.15	<0.15	<0.15	<0.15	0.16	3.37	<0.15	0.15
<2	<7	<7	<7	<7	<7	<2	<2	<2
0.11	0.25	0.24	0.53	0.10	0.10	4.34	9.54	5.18
0.14	<0.06	<0.02	<0.02	<0.04	<0.02	0.16	<0.02	<0.02
<0.02	<0.08	<0.02	<0.02	<0.11	<0.02	7.90	0.07	<0.02
<0.1	<0.1	<0.1	<0.1	<0.2	<0.1	0.78	0.07	<0.05
<0.04	<0.04	<0.04	<0.04	<0.04	<0.04	19.20	0.86	0.47
<1	<1	<1	<1	<1	<1	32.8	1.8	0.7
<1	<1	<1	<1	<1	<1	9.39	<1	<1
<0.01	<0.01	<0.01	0.02	<0.01	<0.01	1.47	0.34	0.18
<0.05	<0.05	<0.05	<0.05	<0.05	<0.05	0.41	0.15	0.11
<0.05	<0.05	<0.05	<0.05	<0.05	<0.05	0.23	0.05	0.05
<0.1	<0.1	<0.1	<0.1	<0.1	<0.1	0.18	0.10	0.00
<0.06	<0.06	<0.06	<0.06	<0.06	<0.06	0.57	0.24	0.15
<0.01	<0.01	<0.01	<0.01	0.01	<0.01	0.09	0.04	0.03
130	21	48	308	48	331	128	380	205
20	155	77	298	84	31	42	96	212
39	401	88	563	774	53	94	138	64
77,039	27,663	29,998	17,798	28,298	29,573	10,868	21,480	17,527
9,898	18,600	7,308	28,000	24,118	650	63,158	53,600	86,735
625	93.2	221	127	119	329	91.3	50.1	54.9
<2	2.5	<2	6.6	8.1	<2	12.5	9.5	15.9
0.7	1.9	0.8	9.4	0.9	0.5	0.8	1.6	2.2
2,086	1,150	1,374	3,251	1,217	1,390	306	543	469
<0.05	0.20	0.25	1.65	0.10	0.06	0.14	0.33	0.11
82.53	55.11	48.71	52.71	58.41	37.68	32.69	37.75	42.38
23	<2	5	<2	4	9	6	11	15
55.28	3.03	16.02	5.79	4.34	26.57	15.62	7.26	13.44
119	<7	62	25	18	75	21	17	44
719	53.4	169	96.9	68.1	229	208	115	132
271	472	52	522	231	228	148	32,769	2,883
7,135	2,814	1,546	4,663	2,996	2,180	2,072	4,571	5,098
58.5	75.5	27.9	157	26.4	4.1	72.3	58.3	104

gn Gabbronorite, *SP* Selebi-Phikwe

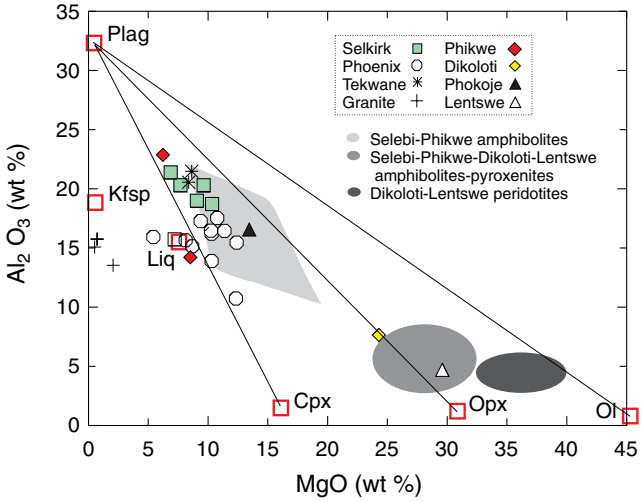

Fig. 3 Binary variation diagram of Al_2O_3 vs MgO. Data of Brown (1988) are shown in *shaded fields*. Mineral compositions were estimated by calculating CIPW norms (Brown 1988). *Liq* Postulated parental magma composition to Selebi-Phikwe intrusions (HGN1 of Brown 1988), *Plag* plagioclase; *Kfsp* K-feldspar, *Cpx* clinopyroxene, *Opx* orthopyroxene, *Ol* olivine

(apart from high Fe_2O_3 caused by the presence of ca 10% injected sulfide) are broadly consistent with the proposed parental liquid composition to the intrusions, indicating that the boulder may represent a fragment from the country rock hornblende gneisses proposed to represent metamorphosed basaltic flows (Brown 1988).

The mantle-normalised lithophile element plots for the samples from the Tati belt are, with the exception of positive anomalies at K, U and between Ba to Cs, flat (Th/Yb_N=1.57). In some cases, Eu is also relatively enriched (Fig. 4b,c). The enrichment in large ion lithophile elements is characteristic of arc basalts (Hawkesworth et al. 1977; Sun 1980; Pearce 1983; Barnes et al. 1993; Fig. 4d) and is normally interpreted as the signature of a subduction component, whereas the flat patterns of the other incompatible trace elements are normally interpreted to reflect magma generation in the depleted oceanic mantle. The samples from the Selebi-Phikwe area show similar positive K, U, and Ba to Cs anomalies as the Tati samples, but in addition, most of the

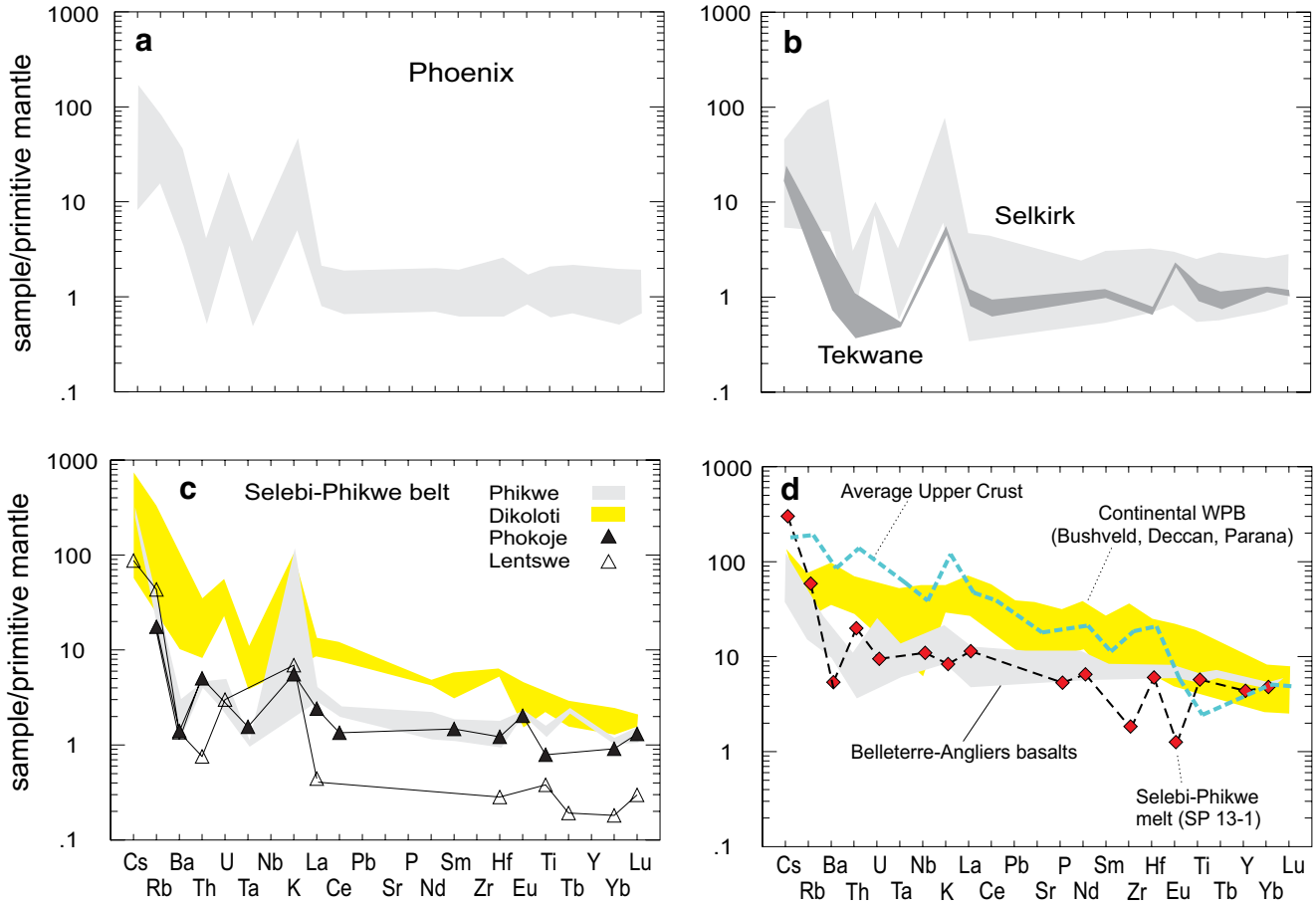

Fig. 4 Mantle normalised lithophile trace element patterns of Botswana Ni deposits (normalisation factors from McDonough and Sun 1995). **a** Phoenix. **b** Selkirk and Tekwane. **c** Deposits of the Selebi-Phikwe belt. **d** Oceanic arc and back arc basalts in the Belleterre-Angliers Belt, Canada (from Barnes et al. 1993) compared to possible melt composition at Phikwe (sample SP13). Also shown are the compositions of average upper crust (Taylor and McLennan 1985) and the field of continental within-plate basalts (data from Barnes and Maier 2002 and Wilson 1989)

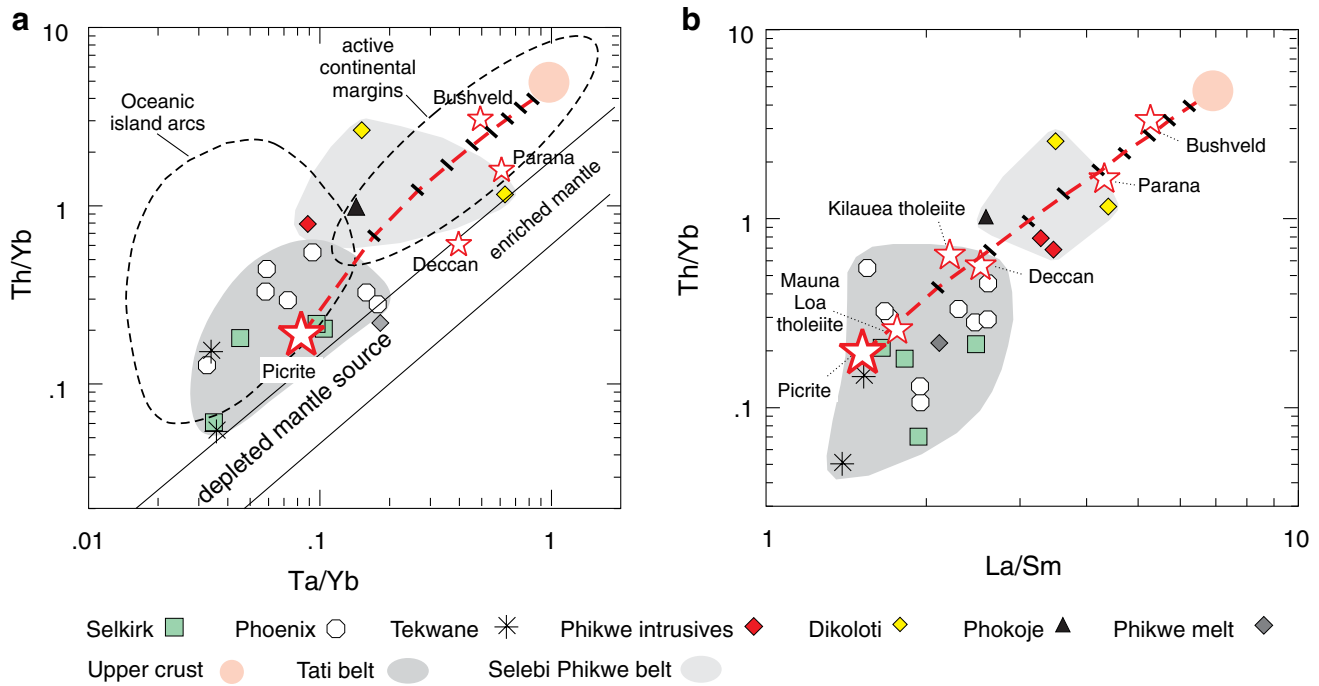

Fig. 5 Binary variation diagram of **a** Th/Yb vs Ta/Yb and **b** Th/Yb vs La/Sm for Tati and Selebi-Phikwe samples with low to intermediate sulfide contents. Fields of oceanic island arcs and active continental margins in **a** are from Pearce (1983). Composition of average upper crust is from Taylor and McLennan (1985), model picrite from Arndt et al. (1993), Mauna Loa, Kilauea, Deccan, Parana and Greenland lavas from Wilson (1989), and Bushveld magnesian basalt from Barnes and Maier (2002). Mixing lines between upper crust and picrite have been calculated assuming bulk mixing

rocks (especially those from Dikoloti) are also relatively enriched in LREE and Th (Th/Yb_N=4.22; Fig. 4c). These features are consistent with the presence of a component from the continental crust (Fig. 4d). Notably, sample SP13-1 has relatively flat trace element patterns that resemble those of the Tati samples.

The compositional differences between the Tati and Selebi-Phikwe samples are highlighted in ratio diagrams of incompatible trace elements (Fig. 5). The Tati samples plot adjacent to model primitive picrite and oceanic island tholeiites and contain <10–20% crustal component. In contrast, the Phikwe and, in particular, the Dikoloti samples plot towards the fields of intra-continental basalts and average upper continental crust and contain >10–20% of upper crust. Sample SP13-1 forms an exception in that it plots with the Tati samples.

Chalcophile elements

In most of the studied deposits, the chalcophile metals show well-defined positive correlations with sulfur in rocks containing disseminated sulfides (Fig. 6), indicating restricted mobility of the metals and sulfur during and after crystallisation of the rocks. The individual deposits define distinct compositional fields in the plots. The samples from Phoenix (and Tekwane) have the highest metal/S ratios, whereas the samples from Selkirk and Phikwe have progressively lower metal/S ratios. Amongst the deposits of the Selebi-Phikwe belt, the samples from Dikoloti have relatively high PGE/S ratios, but relatively low base metal to sulfur ratios. The number of samples from Phokoje and Lentswe is too low to allow the recognition of systematic trends.

The massive sulfide ores (samples with >ca 20–30% S) show more pronounced variation in metal contents than the rocks containing disseminated sulfides, resulting in poor correlations between the metals and sulfur. Variation is particularly pronounced for Cu and PGE contents in the massive ores from Phoenix and, to a lesser degree, Selkirk, indicating fractionation of the metals during the formation of the massive sulfides.

To allow a meaningful comparison of metal contents in the samples, the concentrations of the metals have been normalised to 100% sulfide using the method of Barnes and Lightfoot (2005). The average compositions of individual deposits (and of some distinct types of mineralisation) are given in Table 5. In most deposits, the disseminated sulfide mineralisation is somewhat richer in metals than the massive sulfide ores. In particular, the disseminated mineralisation tends to be relatively enriched in Cu, resulting in higher Cu/Ni ratios, and in Pt, resulting in higher Pt/Pd relative to the massive sulfide ores. As was seen in Fig. 6, the sulfide mineralisation from the Tati belt is systematically enriched in PGE, Ni, Cu, Co and Se relative to the Selebi-Phikwe sulfide mineralisation.

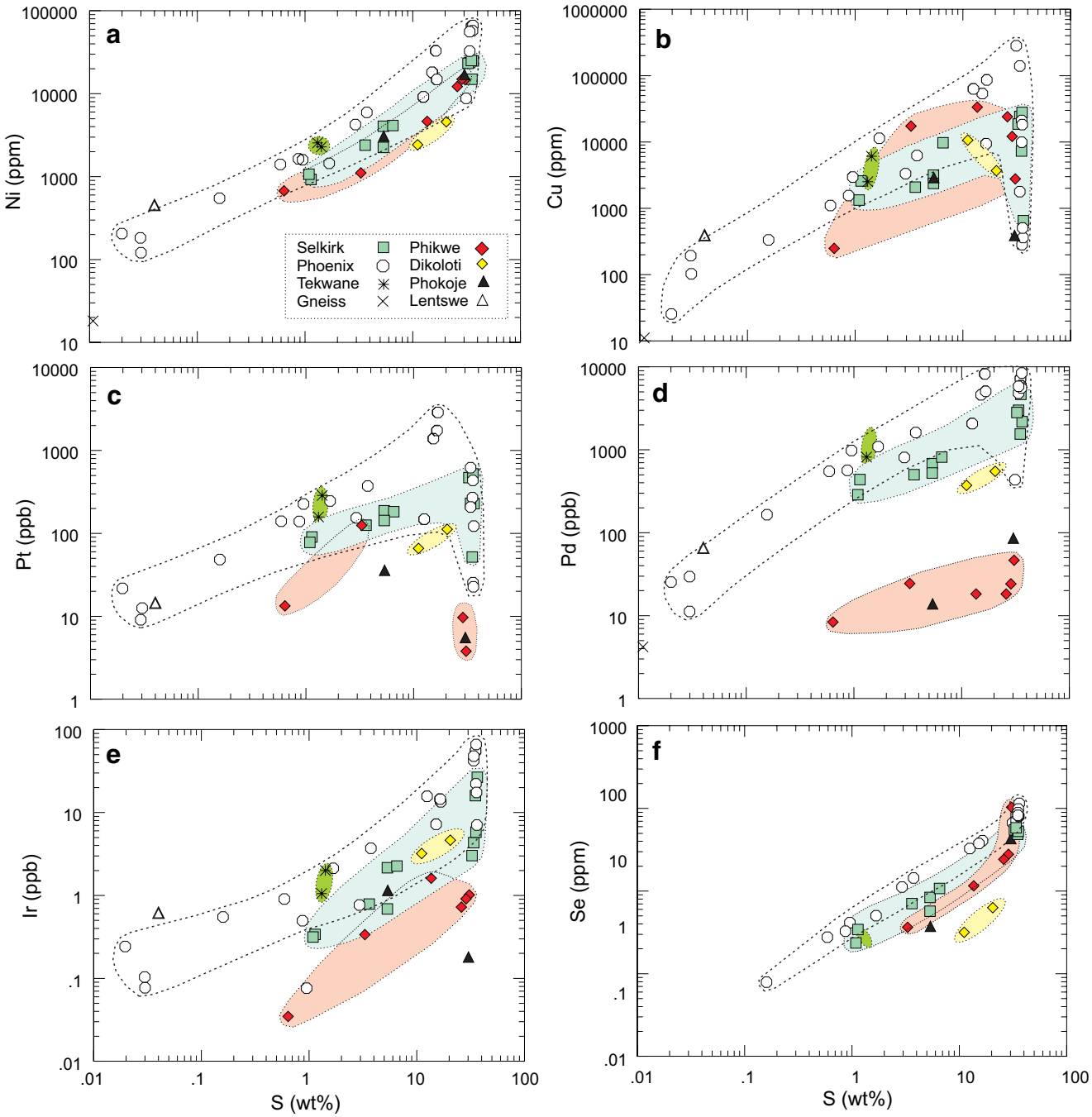

Fig. 6 Binary variation diagrams vs S of **a** Ni, **b** Cu, **c** Pt, **d** Pd, **e** Ir and **f** Se. Individual deposits define distinct compositional fields and massive sulfide ores show more compositional variation than samples containing disseminated sulfides. See text for further explanation

The compositions of the sulfide fractions of the rocks are normalised to primitive mantle in Fig. 7. Some important features may be highlighted: (1) The samples containing disseminated sulfides show a broadly progressive and relatively steep increase in metal concentration from Ir to Cu, i.e. the patterns are strongly fractionated, reflecting the gabbroic nature of the intrusions (e.g. Barnes et al. 1985). The Tati samples (Pd/Ir mostly »100) are systematically more fractionated than the Selebi-Phikwe samples (see also Table 5). (2) Most of the Tati samples have $Cu/Pd_N<1$, whereas most Selebi-Phikwe samples have $Cu/Pd_N>1$. This indicates that the Tati sulfides segregated from magmas that were undepleted in PGE relative to Cu, whereas the Selebi-Phikwe sulfides segregated from strongly PGE-depleted magmas. The Dikoloti samples form an exception within the Selebi-Phikwe belt in that they are undepleted or weakly depleted in PGE relative to Cu and Se. (3) Most samples have $Ni/Ir_N>1$. This may be explained by a higher bulk partitioning of Ir relative to Ni during fractionation of basaltic magmas

Table 5 Average metal contents in the deposits of the Tati and Selebi-Phikwe belts (normalised to 100% sulfides)

	n	% sulf	Ni (wt%)	Cu (wt%)	Ag (ppm)	Co (ppm)	Se (ppm)	Os (ppb)	Ir (ppb)	Ru (ppb)	Rh (ppb)	Pt (ppb)	Pd (ppb)	Au (ppb)	Cu/Ni	Pt/Pd	Pd/Ir
Dikoloti diss sulf	1	27.2	1.06	3.92	11	629	12		15		79	297	1,793	140	3.69	0.17	121
mass sulf	1	51.2	1.07	0.72		669	12		9		74	214	2,144	12	0.67	0.10	238
Phikwe diss sulf	3	13.6	2.90	12.15	45	1,889	44		4		9	1,087	279	442	6.52	2.05	66
mass sulf	3	71.6	2.32	1.93	7	1,093	69		2		5	17	71	36	0.83	0.25	30
Phokoje diss sulf	1	13.3	2.77	2.20		1,425	28		9		16	269	95	33	0.79	2.84	11
mass sulf	1	74.7	2.72	0.05		1,299	58		0		2	20	224	9	0.02	0.09	1554
Phoenix diss sulf	5	10.7	9.13	11.77	44	3,092	158	35	47	478	573	6,668	28,254	1,317	1.26	0.24	580
mass sulf	7	86.8	8.36	0.86		2,142	102	20	45	93	731	298	7,584	55	0.10	0.04	322
Cu-rich sulfides	5	46.9	4.41	25.46	70	1,188	114	30	43	92	488	26,258	8,475	282	8.78	1.57	314
Veins in gneiss	2	4.6	8.10	9.36	127	1,985	180	10	7		398	6,424	28,878	1,039	1.11	0.21	6944
Selkirk diss sulf	6	9.4	3.51	4.60	19	1,946	79		12	77	134	1,912	7,916	357	1.31	0.24	680
mass sulf	5	89.1	2.98	1.79	7	1,902	57	6	12	50	138	340	3,212	67	0.67	0.10	521
Tekwane diss sulf	2	3.0	9.55	14.21		2,544	122		45		585	7,354	37,965	7,152	1.49	0.19	842

diss sulf Disseminated sulfides, *mass sulf* massive sulfides, *n* number of samples, *% sulf* calculated sulfide content (method of Barnes and Lightfoot 2005)

(Crocket 2002). (4) Au shows negative anomalies in most deposits, possibly due to its mobility in fluids. (5) The massive ores from Phoenix show pronounced variation in Cu, Au, Pt and Pd. An almost pure chalcopyrite sample is relatively enriched in Cu, Au and Se, but depleted in all other metals. The Ni-rich ores (average of four samples) are relatively depleted in Cu, Au and, to a lesser degree, Se, but relatively enriched in the other metals.

Discussion

Composition of the parental magmas

Brown (1988) suggested that the intrusions of the Selebi-Phikwe and Tati belts crystallised from tholeiitic basalt containing ca 8% MgO and 15% Al_2O_3. Our lithophile major element data are consistent with a broadly basaltic lineage of all studied intrusions (Fig. 3). The composition of the sulfide mineralisation provides some additional constraints. Nickel (and Ir) behaves in a compatible manner during fractionation of komatiitic and basaltic magmas, whereas Cu (and Pd) is incompatible in the absence of sulfides (e.g. Barnes and Maier 1999; Crocket 2002). As a result, sulfides that segregate from fractionating magmas tend to have progressively higher Cu/Ni (and Pd/Ir) ratios. The Cu/Ni ratios of the sulfide-bearing rocks examined here are mostly between ca 0.1 and 15 (Fig. 8a), and their Pd/Ir ratios are between ca 10 and 1,500 (Fig. 8b). These ratios are in the range of typical sulfide ores formed from basaltic magmas (Barnes et al. 1985; Naldrett 1989; Barnes and Lightfoot 2005) consistent with a basaltic lineage of the Tati and Selebi-Phikwe intrusions. However, the Tati sulfide mineralisation has significantly higher Cu and Ni tenors, suggesting that the intrusions of the two belts are not co-magmatic. This interpretation is supported by our PGE data. (1) The Tati samples have higher Pd/Ir ratios than the Selebi-Phikwe samples (Fig. 8b), implying that the parental magma to the Tati intrusions was slightly more differentiated than that to the Selebi-Phikwe intrusions. (2) The sulfide mineralisation in the Tati belt is significantly more enriched in PGE and has higher PGE/base metal ratios than the sulfide mineralisation in the Selebi-Phikwe belt (Table 5). This indicates that the Tati magmas did not reach S saturation before emplacement, whereas most of the Selebi-Phikwe magmas had equilibrated with sulfide liquid before emplacement.

Figure 9 provides some additional, semi-quantitative constraints. Most of the Tati samples can be explained by sulfide segregation from undepleted oceanic arc tholeiite at R factors (mass ratio of silicate magma to sulfide melt; Campbell and Naldrett 1979) between 100 and 1,000. Most

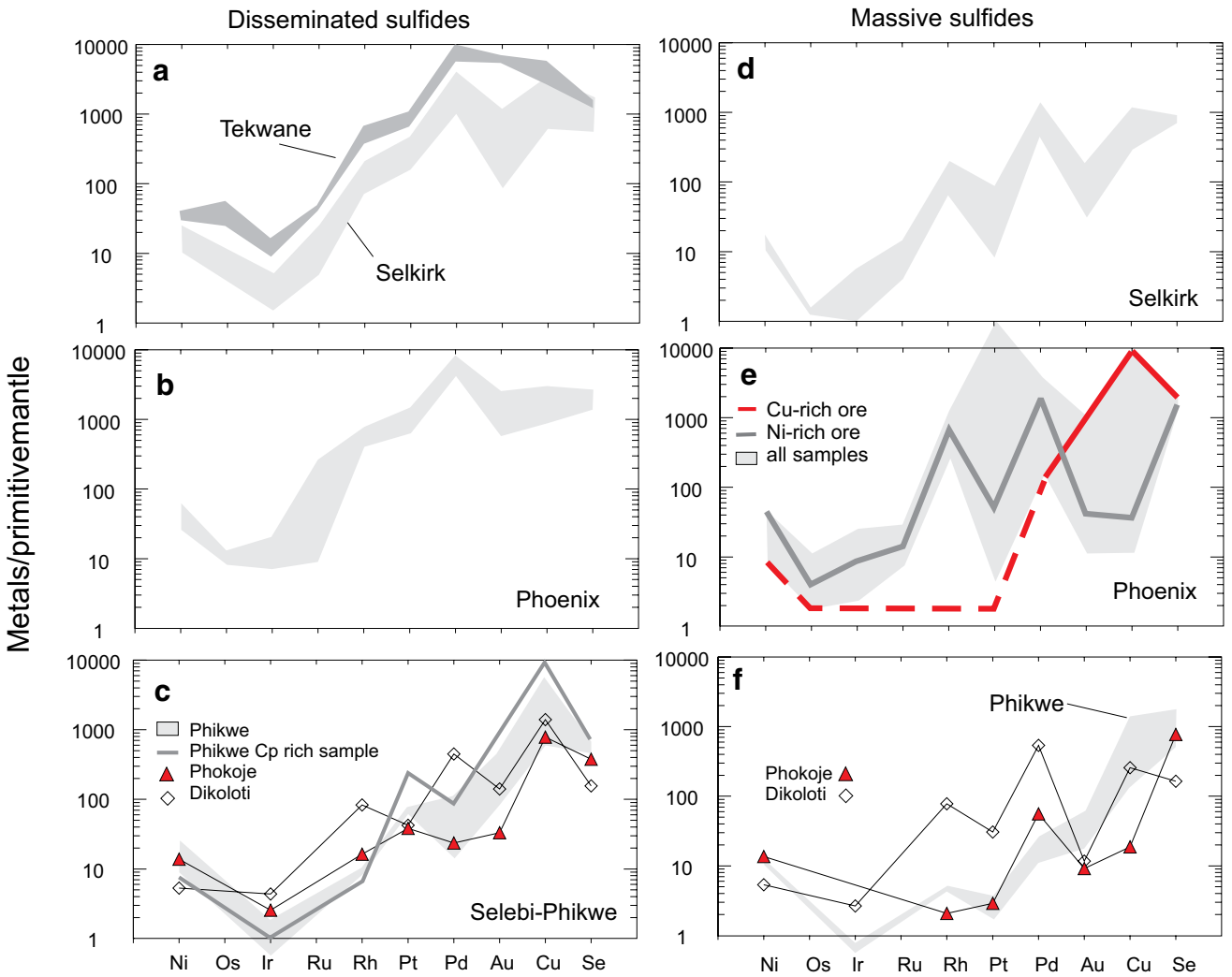

Fig. 7 Primitive mantle-normalised metal patterns (normalisation factors from Barnes and Maier 1999). **a**–**c** Disseminated sulfide mineralisation from Selkirk, Tekwane, Phoenix and Selebi-Phikwe. **d**–**f** Massive sulfide ores from Selkirk, Phoenix and Selebi-Phikwe

of the Selebi-Phikwe samples have much higher Cu/Pd that cannot be modelled by segregation from the undepleted oceanic arc tholeiite. Instead, modelling of the Selebi-Phikwe samples requires a strongly PGE depleted magma. Figure 9 also suggests that the Dikoloti sulfide mineralisation is not co-genetic to that in the other Selebi-Phikwe deposits unless one proposes R factors several orders of magnitude higher than applicable to the Selebi-Phikwe sulfides, a model that seems unrealistic. The composition of the Dikoloti mineralisation is better explained by segregation from moderately depleted magma at relatively low R factors.

Ore formation

(1) Assimilation of external sulfur

Based on mass balance considerations and sulfur isotopic data, many authors feel that the formation of large magmatic sulfide deposits requires assimilation, by the magma, of external sulfur from the country rocks. However, the specific mechanisms of sulfur addition remain controversial (see Barnes and Lightfoot 2005 and references therein). Past authors envisaged bulk or partial assimilation of sulfide-bearing pelitic rocks (e.g. Ripley and Al-Jassar 1987), coupled assimilation of evaporite (adding sulfate to the magma) and coal (reducing the sulfate to sulfide; Naldrett 2004) and migration of sulfur gas from heated sediments to the magma (e.g. Ripley 1981).

The role of external sulfur in the genesis of the Botswana Ni deposits is particularly difficult to constrain. Most of the granitic and gneissic rocks in the Selebi-Phikwe area are relatively sulfur poor (<ca 200 ppm sulfur; Brown 1988). Unless the gneisses lost much of their sulfur during high-grade metamorphism, they cannot have contributed significant external sulfur to the mafic–ultramafic intrusions. Within the Tati belt, some rocks of the Lady Mary and Penhalonga formations, as well as some tonalitic

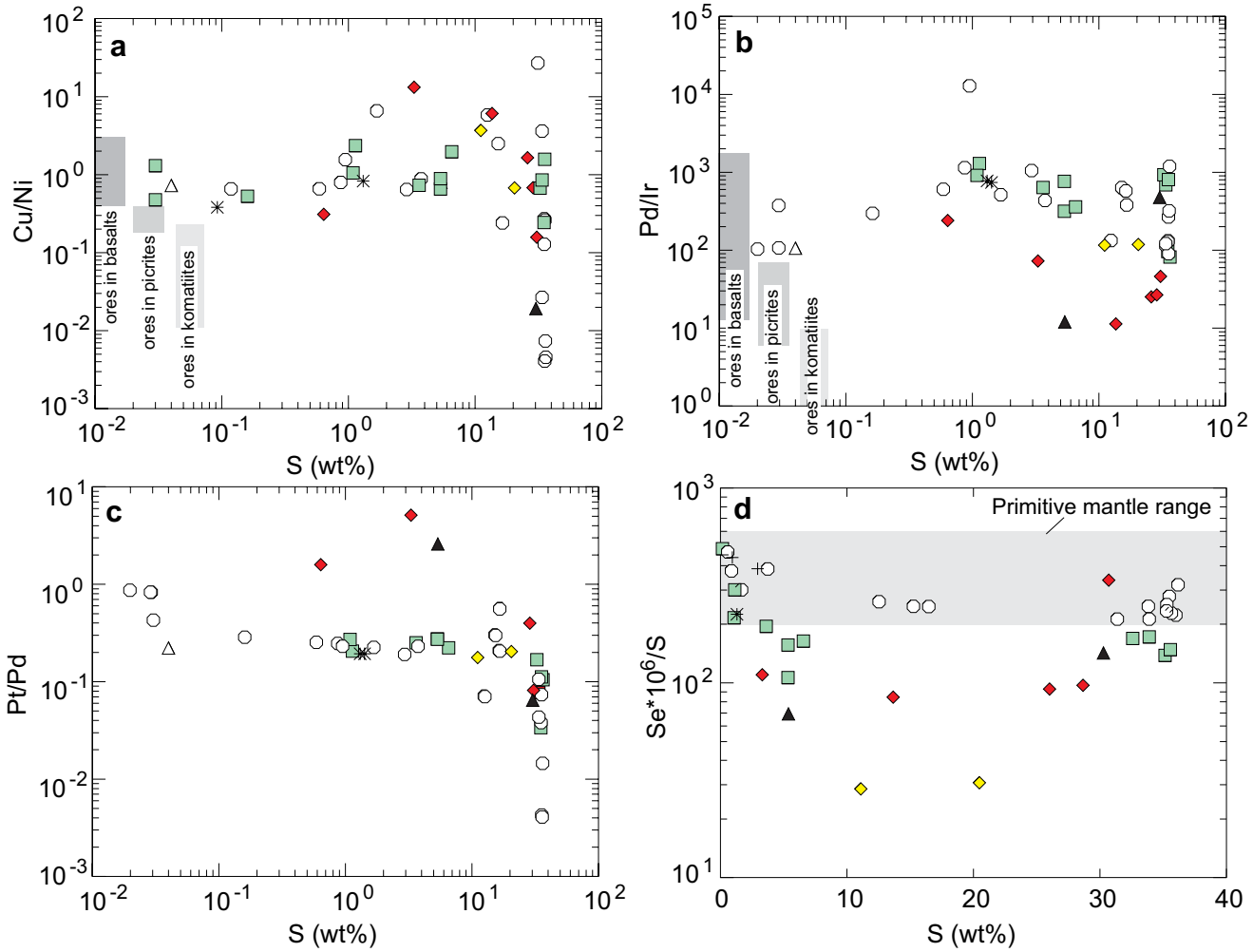

Fig. 8 **a** Cu/Ni vs S, **b** Pd/Ir vs S, **c** Pt/Pd vs S and **d** Se/S vs S. Fields of Cu/Ni and Pd/Ir ores in basalts, picrites and komatiites are from Barnes and Maier (1999), Barnes and Lightfoot (2005) and Naldrett (2004). See Fig. 6 for symbols

paragneisses, contain accessory sedimentary-derived sulfides (Key 1976), but detailed information about sulfide contents in these rocks is presently unavailable. The lithophile trace element signatures of the Tati intrusions provide no direct support for significant contamination of the parental magmas (Figs. 4 and 5). Substantial volatile transfer of sedimentary sulfur from the country rocks to the intrusions is unlikely, as this mechanism requires the migration of fluids against the thermal gradient and through the chilled relatively impermeable contact rocks.

Some workers have tried to constrain the amount of crustal sulfur in magmatic sulfide ores by considering Se/S ratios of the rocks (e.g. Eckstrand et al. 1989). Selenium is a chalcophile element (D 1700; Peach et al. 1990), it occurs at relatively low levels in sedimentary sulfides, and it is immobile. Se/S ratios of mantle rocks are ca 230–350 × 10^{-6}, whereas crustal rocks tend to have Se/S < 50 × 10^{-6} (Eckstrand et al. 1989), although higher values are also observed (e.g. ca 50–400 × 10^{-6} in some Finnish sediments; Peltonen 1995). Thus, sulfide ores containing a large contribution of crustal sulfur tend to have low Se/S ratios at relatively high sulfide contents and low metal tenors (e.g. Peltonen 1995; Thériault and Barnes 1998). Se/S ratios of the Botswana sulfides are plotted against sulfide content in Fig. 8d. The Tati rocks have Se/S ratios in the range 100–500 × 10^{-6}, whereas the Selebi-Phikwe rocks have lower Se/S ranging mostly between 30 and 150 × 10^{-6}. These values are similar to those of some other sulfide-rich Ni–Cu–PGE ores for which external sulfur sources have been implied, e.g. Thompson (40–90), Sudbury (70–600), Vammala (50–350), and komatiite-hosted sulfides in the Abitibi greenstone belt of Canada (5–500; Eckstrand, unpublished data; Vammala data from Peltonen 1995). Moreover, there is a clear trend in our data whereby those deposits that show the most fractionated lithophile trace element signatures (Dikoloti, Phikwe and Phokoje) have the lowest Se/S ratios (Fig.

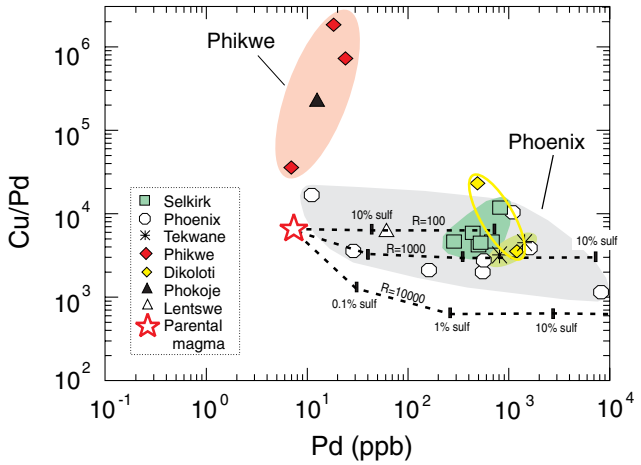

Fig. 9 Cu/Pd vs Pd of samples containing disseminated sulfides in the Tati and Selebi-Phikwe belts. Tie lines are drawn for model sulfides crystallising from metal-undepleted island arc magma (45 ppm Cu, 7.5 ppb Pd; Barnes et al. 1993) at variable R factors, providing a reasonable fit for the deposits in the Tati Belt and Dikoloti. The remainder of the Selebi-Phikwe samples has high Cu/Pd ratios, indicating sulfide segregation from strongly metal depleted magma. See text for further discussion

8d). This pattern suggests the presence of an external sulfur component in the deposits of the Selebi-Phikwe belt.

(2) Concentration of the sulfides

Most of the world's large intrusive Ni–Cu sulfide deposits occur in relatively small, sill- and dyke-like bodies (e.g. Noril'sk, Pechenga, Voisey's Bay, Jinchuan, Kabanga) interpreted to represent magma conduits (Naldrett 2004; Barnes and Lightfoot 2005). The formation of the deposits is normally explained by a model whereby suspended sulfide melt droplets are entrained in fast-flowing silicate magma within the conduits. Changes in flow dynamic conditions, e.g. where the conduits widen or at the exits of the conduits into larger magma chambers, cause the precipitation of the sulfides to form the deposits. Whether the Botswana deposits are equally hosted by magma conduits remains unclear due to insufficient data, poor exposure and variable degrees of tectonism and metamorphism. However, a conduit model would be consistent with the relatively small size of all intrusions and the relatively large proportion of sulfides to silicates, particularly at Selebi-Phikwe, and possibly at Phoenix and Selkirk.

Modification of the sulfides during metamorphism and deformation

The massive sulfide ores analysed in the present study, most notably those from Phoenix, show wide variation in metal concentrations (Figs. 6, 7 and 8) reflecting the presence of pentlandite- and chalcopyrite-rich samples. Compositional heterogeneity is a common phenomenon in many sulfide ore deposits and has often been attributed to fractional crystallisation of sulfide liquid (e.g. Barnes and Lightfoot 2005). The process may result in cumulates of monosulfide solid solution that are relatively enriched in Ni, Os, Ir, Ru and Rh and residual liquids that are relatively enriched in Cu, Au, Pt and Pd. Evidence for localised fractionation of sulfide liquid can be observed in some of the Botswana Ni deposits, e.g. in sample SP13-1 from Phikwe where chalcopyrite with high Cu, Pt, Pd and Au contents has infiltrated an amphibolite boulder (Fig. 2e, Table 4). However, in most of our samples, a model of sulfide melt fractionation is inconsistent with the observed metal distributions because the Cu-rich rocks are strongly depleted in Pd and Pt relative to the Ni-rich rocks.

The discrepancy between the compositions of the present samples and other sulfide ores from elsewhere thought to have formed in response to mss fractionation is illustrated in Fig. 10. In theory, fractionating sulfide melts segregating from fertile oceanic island arc basalt should form sulfides whose compositions plot between mss cumulates (characterised by relatively high Ni/Pd and low Cu/Ir ratios) and residual liquids (characterised by relatively low Ni/Pd and high Cu/Ir ratios). Instead, the data from the Tati belt show a restricted range in Pd/Ir at highly variable Cu/Ni. The

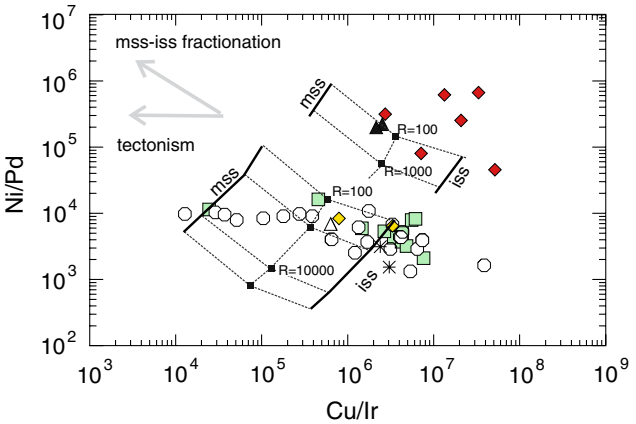

Fig. 10 Binary metal ratio diagram of Ni/Pd vs Cu/Ir. The *stippled grids* indicate range of model compositions of mss and iss mixtures crystallising from fractionating sulfide liquids (assuming sulfide melt/silicate melt D values of 30,000 for the PGE, 1,000 for Cu and 500 for Ni). The mss and iss end members (indicated by *solid lines*) have been calculated by assuming 50% fractional crystallisation of the sulfide liquid and using mss/sulfide melt D values of Barnes et al. (1997). The *lower grid* applies to the Tati sulfides and was calculated assuming a parental silicate magma with 45 ppm Cu, 140 ppm Ni, 7.5 ppb Pd and 0.07 ppb Ir (island-arc magma of Barnes et al. 1993). The grid for the Selebi-Phikwe sulfides (only partly shown for clarity) was calculated assuming 0.1% sulfide extraction from the island arc magma. Note that Tati sulfides show a relatively restricted range in Ni/Pd, but a large variation in Cu/Ir. Mss fractionation would be expected to result in data distribution along *stippled lines* between mss cumulates and iss residues. See text for further explanation. See Fig. 6 for symbols

number of data points from Selebi-Phikwe is too limited to identify distinct trends.

The metal distributions in the Tati ores can be understood by considering Laser-ICP data of magmatic sulfides from Phoenix (Van Geffen 2004). These data indicate that most of the Pd is hosted in pentlandite, whereas the bulk of the Os, Ir, Ru and Rh are hosted in pyrrhotite. Chalcopyrite has low concentrations of all PGE. Platinum is not accommodated by any of the base metal sulfides and may form PGM. As Pd is incompatible with regard to mss and iss (Barnes et al. 1997; Peregoedova 1998), the metal must have diffused from late crystallising magmatic sulfides into the pentlandite. As pentlandite exsolves from pyrrhotite at ca 600°C (Cabri 1992), the diffusion must have occurred below ca 600°C. At this stage, the various magmatic sulfide minerals were apparently still in physical contact. The formation of distinct Ni- and Pd-rich and Cu-rich massive sulfides must have occurred later, possibly in response to tectonism during granite intrusion. Magmatic sulfides behave in a variably ductile manner in a stress regime (Vokes 1969). Ductility decreases from chalcopyrite through pyrrhotite to pentlandite. As a result, tectonised ore bodies can have relatively chalcopyrite-, pyrrhotite- and pentlandite-rich portions (Barrett et al. 1977). The relatively undeformed nature of the silicate host rocks to the ores (Fig. 2a) can be explained by the fact that the silicate rocks are brittle, and hence, will behave more competently than the sulfides. This can result in large blocks of undeformed gabbro and occasional narrow shear zones in the gabbro where the deformation has been absorbed.

Geotectonic setting

The lithophile trace element patterns of the Tati intrusions suggest that they were emplaced in an oceanic arc setting (Fig. 4a,b). Basaltic magmas with island-arc affinities similar to those at Tati have also been identified in the Northern Marginal Zone of the Limpopo Belt (Rollinson and Lowry 1992) and in 2.7 Ga greenstone belts of the Zimbabwe craton (Hawkesworth and O'Nions 1977). The intrusions of the Selebi-Phikwe belt, notably at Dikoloti, contain a larger crustal component than the Tati intrusions, as indicated by more fractionated trace element patterns (Figs. 4c and 5). The relatively enhanced crustal component could have been acquired at the magmatic stage, e.g. by melting of metasomatised subcontinental lithospheric mantle, by contamination of mantle magma during ascent through a mature oceanic arc (as proposed for Indonesian island-arc magmas; Whitford and Jezek 1982) or by contamination of mantle magma during ascent through continental crust (e.g. Thompson et al. 1984). Alternatively, the enhanced crustal component in the Selebi-Phikwe rocks could reflect tectonic mingling of island-arc mafic intrusions with their host rocks, as suggested by the abundance of gneissic fragments in the intrusions (Fig. 2e,f). The latter interpretation is supported by the fact that the trace element ratios of one of the Selebi-Phikwe samples (amphibolite boulder SP13-1 from Phikwe; Fig. 2e) are indistinguishable from those at Tati (Fig. 5).

Our interpretation differs from that of Light (1982), Burke et al. (1985), Kampunzu et al. (2003) and McCourt et al. (2004) who proposed an essentially Andean-type paleotectonic environment for both the Tati and Selebi-Phikwe belts based largely on the composition of granitic rocks. A possible explanation that could reconcile the contrasting models is that the mafic–ultramafic intrusions represent an early oceanic stage in the evolution of the arc, whereas the calcalkaline granitic rocks formed when the arcs had matured and underwent partial melting at their bases. High-precision age determinations of the various intrusive rocks are required to constrain this model, but in the case of the most tectonised mafic intrusions, notably at Selebi-Phikwe, this will be a challenging task.

Implications for exploration

Most of the world's large magmatic sulfide deposits are interpreted to have formed in oceanic or continental rift settings. Such tectonic environments are characterised by vast volumes of relatively Ni-rich magma generated during relatively large degrees of melting in a mantle plume (Campbell 2005). Intersection of the plume with a rift allows the magma to ascend relatively fast to the upper crust without undergoing substantial differentiation en route that might result in sulfur saturation and metal depletion. The emplacement of large amounts of magma in the upper crust will heat the country rocks and may ultimately result in significant assimilation of the country rocks by the magmas.

Orogenic settings have so far attracted relatively little exploration effort based partly on theoretical considerations. Most mantle magmas in orogenic settings form by flux melting of mantle wedges overlying subduction zones. The process probably results in relatively lower volumes of mantle-derived magmas, and in less primitive magma compositions, than adiabatic melting of a mantle plume. Furthermore, the predominantly compressive environments of orogenic belts may result in relatively few dilatant sites through which magmas can ascend, and orogenic belts tend to contain fewer S-bearing sedimentary strata than rifts (Mitchell and Garson 1981).

Until recently, this exploration model seemed consistent with empirical observations, i.e. most magmatic sulfide deposits in plate margin settings are relatively small. Examples that come to mind are those in the Early Devonian Appalachian orogenic belt of North America (e.g. St Stephen, ca 1 mt at 1.05% Ni, 0.53% Cu; Paktunc

1990), the Silurian-Devonian Caledonide orogenic belt of Norway (e.g. the Bruvann deposit in the Råna intrusion, 43 mt at 0.33% Ni; Boyd and Mathiesen 1979) and the Early Proterozoic Vammala belt of Finland (combined 7.5 Mt at 0.66% Ni and 0.42% Cu; Peltonen 1995). However, evidence for an enhanced sulfide potential of magmatic arc settings has begun to accumulate in the last two decades with the discovery of Ni–Cu ores in the Early Proterozoic Sally Malay intrusion of Australia (ca 4 Mt at 1.8% Ni and 0.73% Cu; Hoatson and Blake 2000) and the Early Carboniferous Aguablanca intrusion of Spain (16 Mt at 0.66% Ni and 0.46% Cu; Pina et al. 2006). The identification of an increasing number of sizeable magmatic Ni–Cu ore deposits in orogenic environments (including the Selebi-Phikwe and Tati belts) suggests that the currently used exploration models for such deposits are incomplete and that many orogenic belts should be revisited with regard to their Ni–Cu potential. Of particular exploration interest are transtensional zones that may allow mantle magmas to ascend to upper crustal levels.

Summary and conclusions

1. Most of the Botswana intrusions studied by us are of a gabbronoritic composition. Troctolites, pyroxenites and peridotites also occur but are less abundant. The Tati intrusions are located in the upper portions of a 2.6–2.7 Ga greenstone belt. Due to intense tectonism, the age and paleotectonic setting of the Selebi-Phikwe intrusions are less clear, but may be broadly analogous to Tati.
2. The lithophile trace element data of the Tati intrusions indicate that they formed in an oceanic island arc setting and have not assimilated significant amounts of upper crust during emplacement. The Selebi-Phikwe intrusions, in particular Dikoloti, have a more variable but generally higher crustal component than the Tati intrusions, as suggested by higher Th/Yb, Ta/Yb and La/Sm ratios. However, this is, at least partly, the result of tectonically introduced country rock fragments, raising the possibility that the Selebi-Phikwe magmas were also emplaced in an island arc setting. The data, thus, suggest that orogenic belts are more prospective for Ni deposits than presently recognised.
3. The trigger for sulfide saturation in both the Tati and the Selebi-Phikwe belts remains unclear. The country rocks to the intrusions are generally sulfur poor, but in some deposits (notably Dikoloti and Phikwe), there is a strong correlation between low Se/S ratios and fractionated trace element ratios, suggesting that the magma assimilated S-bearing crustal rocks. The mechanisms leading to the concentration of the sulfides also remain unclear. However, all studied intrusions are relatively small, and many have high mass ratios of sulfides to silicates consistent with sulfide precipitation in flow dynamic traps within magma conduits.
4. The Tati and Selebi-Phikwe deposits show systematically different metal contents, indicating that they are not co-genetic. The composition of the sulfide mineralisation in the Tati rocks is relatively Ni- and PGE-rich and shows high Pd/Ir (»100), indicating crystallisation from a fertile relatively differentiated basalt. The composition of the sulfide mineralisation in most Selebi-Phikwe samples shows lower Ni and PGE contents and Pd/Ir ratios (<100), suggesting equilibration of less differentiated basalt with sulfides before emplacement.
5. The sulfide mineralisation at Dikoloti has lower Ni and Cu contents, but higher PGE contents than at Phikwe. This cannot be explained by variation in R factor, but suggests that the Dikoloti and Phikwe sulfides are not co-genetic and that the intrusions do not form part of the same tectonically dismembered sill.
6. The Phoenix ores formed in response to mobilisation of disseminated sulfides possibly during intrusion of Late Proterozoic granites. The ores appear to have behaved in a variably ductile manner during deformation, resulting in fractionation of Ni-rich from Cu-rich sulfides. The Ni-rich ores are relatively enriched in Os, Ir, Ru, Rh and Pd, whereas the most Cu-rich ores are depleted in all PGE.

Acknowledgements We thank Tati Nickel for facilitating sampling of the Phoenix and Selkirk deposits and for allowing publication of the data. Richard Lewis, Admore Botepe and Kebalemogile Tau assisted WM and GC during the fieldwork. Falconbridge Ventures of Africa allowed sampling at Tekwane. The analytical work was partly funded by the Centre for Research on Magmatic Ore Deposits at the University of Pretoria (to WDM) and NSERC (to SJB). Peter Lightfoot and an anonymous reviewer provided detailed reviews that greatly improved earlier versions of this paper. Additional suggestions for improvement were made by Larry Meinert.

References

Arndt NT, Czamanske GK, Wooden JL, Fedorenko VA (1993) Mantle and crustal contributions to continental flood volcanism. Tectonophysics 223:39–52

Bagai Z, Armstrong RA, Kampunzu AB (2002) U-Pb single zircon geochronology of granitoids in the Vumba granite-greenstone terrain (NE Botswana): implications for the evolution of the Archean Zimbabwe craton. Precambrian Res 118:149–168

Baldock JW, Hepworth JV, Marengwa BS (1976) Gold, base metals, and diamonds in Botswana. Econ Geol 71:139–156

Barnes S-J, Lightfoot PC (2005) Formation of magmatic nickel sulfide ore deposits and processes affecting their copper and platinum-group element contents. Economic Geology 100th Anniversary Volume. Denver, pp 179–213

Barnes S-J, Maier WD (1999) The fractionation of Ni, Cu and the noble metals in silicate and sulphide liquids. In: Keays RR, Lesher CM, Lightfoot PC, Farrow CEG (eds) Dynamic processes in magmatic ore deposits and their application to mineral exploration. Geological Association of Canada, Short Course Notes 13:69–106

Barnes S-J, Maier WD (2002) Platinum-group elements and microstructures of normal Merensky Reef from Impala Platinum Mines, Bushveld Complex. J Petrol 43:103–128

Barnes S-J, Naldrett AJ, Gorton MP (1985) The origin of the fractionation of platinum-group elements in terrestrial magmas. Chem Geol 53:303–323

Barnes S-J, Couture J-F, Sawyer EW, Bouchaib C (1993) Nickel–copper occurrences in the Belleterre-Angliers belt of the Pontiac Subprovince and the use of Cu–Pd ratios in interpreting platinum-group element distributions. Econ Geol 88:1402–1419

Barnes S-J, Makovicky E, Makovicky M, Rose-Hansen J, Karup-Moller S (1997) Partition coefficients for Ni, Cu, Pd, Pt, Rh and Ir between monosulfide solid solution and sulphide liquid and the formation of compositionally zoned Ni–Cu sulphide bodies by fractional crystallization of sulfide liquid. Can J Earth Sci 34:366–374

Barrett FM, Binns RA, Groves DI, Marston RJ, McQueen, KG (1977) Structural history and metamorphic modification of Archean volcanic-type nickel deposits, Yilgarn Block, Western Australia. Econ Geol 72:1195–1223

Barton JM, Klemd R, Zeh A (2006) The Limpopo Belt: a result of Archean to Proterozoic, Turkic-type orogenesis? In: Reimold WU, Gibson RL (eds) Processes on the Early Earth. Geological Society of America Special Paper 405, pp 315–332

Bédard P, Barnes S-J (2002) A comparison of the capacity of FA-ICP-MS and FA-INAA to determine platinum-group elements and gold in geological samples. J Radioanal Nucl Chem 254:319–329

Boyd R, Mathiesen CO (1979) The nickel mineralization of the Rana mafic intrusion, Nordland, Norway. Can Mineral 17:287–298

Brown PJ (1988) Petrogenesis of Ni–Cu ore bodies, their host rocks and country rocks at Selebi-Phikwe, eastern Bostswana. Ph.D. thesis, University of Southampton, UK, p 333

Burke K, Kidd WSF, Kusky T (1985) Is the Ventersdorp rift system of southern Africa related to a continental collision between the Kaapvaal and Zimbabwe cratons at 2.64 Ga ago? Tectonophysics 115:1–24

Cabri LJ (1992) The distribution of trace precious metals in minerals and mineral products. Mineral Mag 384:289–308

Campbell IH (2005) Large igneous provinces and the mantle plume hypothesis. Elements 1:265–269

Campbell IH, Naldrett AJ (1979) The influence of silicate:sulfide ratios on the geochemistry of magmatic sulfides. Econ Geol 74:1503–1505

Carney JN, Aldiss DT, Lock NP (1994) The geology of Botswana. Geological Survey of the Botswana Bulletin 37, 113 pp

Crocket JH (2002) Platinum-group element geochemistry of mafic and ultramafic rocks. Canadian Institute Mining Metallurgy and Petroleum, special volume 54, pp 177–210

Eckstrand OR, Grinenko LN, Krouse HR, Paktunc AD, Schwann PL, Scoates RFJ (1989) Preliminary data on sulphur isotopes and Se/S ratios, and the source of sulphur in magmatic sulphides from the Fox River Sill, Molson Dykes, and Thompson nickel deposits, northern Manitoba. In Current Research Part C, Geological Survey of Canada, Paper 89-1C, pp 235–242

Falconbridge Ventures of Africa (1998) Summary report of the results from PL 96/93. Unpublished company report, p 12

Gallon ML (1986) Structural re-interpretation of the Selebi-Phikwe nickel–copper sulphide deposits, eastern Botswana. In: Anhaeusser CR, Maske S (eds) Mineral deposits of Southern Africa. Geological Society of South Africa, pp 1663–1669

Gordon PSL (1973) The Selebi-Pikwe nickel–copper deposits, Botswana. In: Lister LA (ed) Symposium on granites, gneisses and related rocks. Special Publication, Geological Society of South Africa 3:167–187

Hawkesworth CJ, O'Nions RK (1977) The petrogenesis of some volcanic rocks from southern Africa. J Petrol 18:487–520

Hawkesworth CJ, O'Nions RK, Pankhurst RJ, Hamilton PJ, Evensen NM (1977) A geochemical study of island arc and back-arc tholeiites from the Scotia Sea. Earth Planet Sci Lett 36:253–262

Hoatson DM, Blake DH (2000). Geology and economic potential of the Palaeoproterozoic layered mafic-ultramafic intrusions in the East Kimberley, Western Australia. Australian Geological Survey Organization, Bulletin 246:469

Johnson RS (1986) The Phoenix and Selkirk nickel–copper sulphide ore deposits, Tati Greenstone Belt, eastern Botswana. In: Anhaeusser CR, Maske S (eds) Mineral deposits of Southern Africa. Geological Society of South Africa, pp 243–248

Kampunzu AB, Tombale AR, Zhai, M, Bagai Z, Majaule TM, Modisi M (2003) Major and trace element geochemistry of plutonic rocks from Francistown, NE Botswana: evidence for neo-Archean continental active margin in the Zimbabwe craton. Lithos 71:431–460

Key RM (1976) The geology of the area around Francistown and Phikwe, northeast and central districts, Botswana. Distr Mem Geol Surv Botswana 3:15–25

Lear PA (1979) The ore mineralogy of the Phikwe and Selebi nickel–copper deposits, Botswana. Geological Society of South Africa, Special Publication 5:117–132

Light MPR (1982) The Limpopo mobile belt: a result of continental collision. Tectonics 1:325–342

Maier WD (2005) Platinum-group element (PGE) deposits and occurrences: mineralization styles, genetic concepts, and exploration criteria. J Afr Earth Sci 41:165–191

Marsh SCK (1978) Nickel-copper occurrences at Dikoloti and Lentswe, eastern Botswana. In: WJ Verwoerd (ed) Mineralization in metamorphic terranes, Geological Society of South Africa, Special Publication 4:131–148

McCourt S, Kampunzu AB, Bagai Z, Armstrong RA (2004) The crustal architecture of Archean terranes in Northeastern Botswana. S Afr J Geol 107:147–158

McDonough WF, Sun S-S (1995) The composition of the Earth. Chem Geol 120:223–253

Mitchell AHG, Garson MS (1981) Mineral deposits and global tectonic settings. Academic, London, p 405

Naldrett AJ (1989) Magmatic sulphide deposits. Oxf Monogr Geol Geophys 14:186

Naldrett AJ (2004) Magmatic sulfide deposits. Springer, Berlin Heidelberg New York, p 727

Paktunc AD (1990) Comparative geochemistry of platinum-group elements of nickel-copper sulfide occurrences associated with mafic-ultramafic intrusions in the Appalachian orogen. J Geochem Explor 37:101–111

Peach CL, Mathez EA, Keays RR (1990) Sulfide melt-silicate melt distribution coefficients for noble metals and other chalcophile elements as deduced from MORB: implications for partial melting. Geochim Cosmochim Acta 54:3379–3389

Pearce JA (1983) The role of sub-continental lithosphere in magma genesis at destructive plate margins. In: CJ Hawkesworth and MJ Norry (eds) Continental basalts and mantle xenoliths. Shiva, Nantwich, pp 230–249

Peltonen P (1995) Magma-country rock interaction and the genesis of Ni–Cu deposits in the Vammala nickel belt, SW Finland. Mineral Petrol 52:1–24

Peregoedova AV (1998) The experimental study of Pt–Pd partitioning between monosulfide solid solution and Cu–Ni sulfide melt at 900–840°C. In: 8th International Platinum Symposium,

Abstracts, Geological Society of South Africa and S Afr Inst Min Metall, Symposium Series S18, pp 325–327
Pina R, Lunar R, Ortega L, Gervilla F, Alapieti T, Martinez C (2006) Petrology and geochemistry of mafic-ultramafic fragments from the Aguablanca Ni–Cu ore breccia, southwest Spain. Econ Geol 101:865–881
Ripley EM (1981) Sulfur isotopic studies of the Dunka Road Cu–Ni deposit, Duluth Complex, Minnesota. Econ Geol 76:610–620
Ripley EM, Al-Jassar TJ (1987) Sulfur and oxygen isotope studies of melt-country rock interaction, Babbitt Cu–Ni deposit, Duluth Complex, Minnesota. Econ Geol 82:87–107
Rollinson HR, Lowry D (1992) Early basic magmatism in the evolution of the Northern Marginal Zone of the Archean Limpopo Belt. Precambrian Res 55:33–45
Steele TW, Levin J, Copelowitz I (1975) Preparation and certification of a reference sample of a precious metal ore—Report No 1696-1975 of the National Institute of Metallurgy, South Africa, pp 4
Sun S-S (1980) Lead isotopic study of young volcanic rocks from mid-ocean ridges, ocean islands and island arcs. Philos Trans R Soc Lond A297:409–445
Taylor ST, McLennan SM (1985) The continental crust: its composition and evolution. Blackwell, Oxford, p 312
Thériault RD, Barnes S-J (1998) Compositional variations in Cu–Ni–PGE sulfides of the Dunka Road deposit, Duluth Complex, Minnesota: the importance of combined assimilation and magmatic processes. Can Mineral 36:869–886
Thompson RN, Morrison MA, Hendry GL, Parry SJ (1984) An assessment of the relative roles of crust and mantle in magma genesis: an elemental approach. Philos Trans R Soc Lond, A310:549–590
Van de Wel L, Barton JM Jr, Kinny PD (1998) 1.02 Ga granite magmatism in the Tati–granite–greenstone Terrane of Botswana: implications for mineralization and terrane evolution. S Afr J Geol 101:67–72
Van Geffen PWG (2004) Geochemistry of the Phoenix Ni–Cu–PGE deposit, Francistown, Botswana. MSc thesis, Utrecht University, pp 88
Vokes FM (1969) A review of the metamorphism of sulphide deposits. Earth Sci Rev 5:99–143
Wakefield J (1976) The structural and metamorphic evolution of the Phikwe Ni–Cu sulfide deposit, Selebi-Phikwe, eastern Botswana. Econ Geol 71:988–1005
Whitford DJ, Jezek PA (1982) Isotopic constraints on the role of subducted sialic material in Indonesian island-arc magmatism. Bull Geol Soc Am 93:504–513
Wilson M (1989) Igneous petrogenesis. Chapman and Hall, London, p 466
Wright L (1977) A structural cross section across the north margin of the Limpopo Belt. Ph.D. thesis, University of Leeds, UK